

**Non-fibril Amyloid Aggregation at the Air/Water Interface: Self-adaptive
Pathway Resulting in a 2D Janus Nanofilm**

Supporting information

Hao Ren¹⁺, Huan Chen²⁺, Yu Kang³⁺, Wei Liu¹, Yongchun Liu¹, Fei Tao¹, Shuting Miao¹, Yingying Zhang¹, Qian Liu⁴, Mingdong Dong⁴, Yonggang Liu^{3*}, Bing Liu^{2*}, and Peng Yang^{1*}

¹ Key Laboratory of Applied Surface and Colloid Chemistry, Ministry of Education; Xi'an Key Laboratory of Polymeric Soft Matter; International Joint Research Center on Functional Fiber and Soft Smart Textile, School of Chemistry and Chemical Engineering, Shaanxi Normal University, Xi'an 710119, China

² First Affiliated Hospital, School of Medicine, Xi'an Jiaotong University, Xi'an, 710061, China

³ State Key Laboratory of Polymer Physics and Chemistry, Changchun Institute of Applied Chemistry, Chinese Academy of Sciences, Changchun, 130022, China

⁴ Interdisciplinary Nanoscience Center (iNANO), Aarhus University, Aarhus C, Denmark

*Corresponding Author(s): Bing Liu: bliu2018@xjtu.edu.cn; Yonggang Liu: yonggang@ciac.ac.cn; Peng Yang: yangpeng@snnu.edu.cn.

+These authors contributed equally to this work

Experimental section

1. Materials

Hen egg-white lysozyme, thioflavin T (ThT), 1-anilinoanthracene 8-sulfonate (ANS), and N-(1-pyrenyl) maleimide (NPM) were purchased from Sigma-Aldrich. Tris (2-carboxyethyl) phosphine hydrochloride (TCEP) was purchased from TCI. Sinapic acid and trifluoroacetic acid was purchased from Sigma-Aldrich. Ultrapure water was used in all experiments and was supplied by Milli-Q Advantage A10 (Millipore, USA). Silver nanoparticles (AgNPs) for surface-enhanced Raman spectroscopy (SERS) were prepared according to previously reported methods.¹ Mica discs for in-situ AFM measurement were purchased from SPI-CHEM (USA). The Silicon wafer for the AFM test and quartz slice for CD analysis was cleaned with piranha solution before use.

2. Characterization

Atomic force microscope (AFM) was measured by a Dimension ICON (Bruker, USA) with SCANASYST-AIR tip in the air; High-resolution field-emission scanning electron microscopes (FE-SEM) measurement was performed on a SU8220 (Hitachi, Japan) at an accelerating voltage of 5-10 kV; Nuclear magnetic resonance (NMR) experiments were measured by a Bruker 600MHz (Avance III) spectrometer; In-situ AFM analysis was measured by a Cypher VRS (Oxford Instruments, UK) with BL-AC40TS tip (Olympus, Japan) on a 3 mm mica discs (SPI-Chem, USA); AFM adhesion test was performed on Cypher VRS (Oxford Instruments, UK) with SiO₂ particle sensor (CP-FM-SiO₂, diameter 3.5 μm, frequency, 45-115 kHz, force constant, 0.5-9.5 N/m). X-ray photoelectron spectroscopy (XPS) was analyzed by AXIS ULTRA (Kratos), the binding energies were calibrated by setting C1s peak at 284.6 eV; Far-UV Circular Dichroism (CD) spectrum was carried out with a Chirascan (Applied Photophysics, UK); Quartz crystal microbalance (QCM-D) was analyzed using a Q-Sense Explorer from Biolin (Sweden); Surface plasmon resonance (SPR) was measured by a Biacore T200 system (GE Healthcare, Sweden); Contact angle tests were carried out with an OCA 20 from Dataphysics instruments, Germany; Fluorescence analysis were performed using a fluorophotometer F-7000 (Hitachi, Japan); Transmission electron microscope (TEM) was measured with Tecnai G2 F20 (FEI, USA); Asymmetric flow field-flow fractionation (AF4) was measured by Wyatt Eclipse DualTec system (Dernbach, Germany) equipped with a DAWN HELEOS-II (Santa Barbara, CA) multi-angle laser light scattering (MALLS) detector; Young's modulus of the Janus nanofilm was measured by Hysitron TI 980 Nanoindenter (Bruker, USA); surface-enhanced Raman spectroscopy (SERS) was measured on a inVia Reflex Confocal Raman Spectrometer (Renishaw, UK) equipped with 532 nm laser. Matrix-assisted laser desorption/ionization time-of-flight mass spectrometry (MALDI-TOF-MS) was measured by Microflex (Bruker). Time-of-flight secondary ion mass spectrometry (TOF-SIMS) was carried out on a TOF.SIMS-5 (IONTOF, Germany), Bi liquid metal was used as ion source, and the electric current was set at 1pA, and collect 5 points for each sample, and the collect number was 20 times for each point; The shear adhesion test was performed on UTM 2103 mechanical test machine (Shenzhen Suns Technology Stock Co., LTD, China); The Young's modulus from the tensile test was performed on IBTC-100 tensile testing machine (CARE Measure & Control Co., Ltd. China). Grazing-incidence small-angle X-ray scattering (GISAXS) and grazing-incidence wide-angle X-ray scattering (GIWAXS) analysis were carried out at Shanghai Synchrotron Radiation Facility (SSRF), beamline BL16B1 and BL14B1, respectively. The thickness of the self-assembled nanofilm was

characterized by an ALPHA-SE ellipsometer (J.A. WOOLLAM, USA) on silicon substrates.

N-(1-pyrenyl) maleimide (NPM) binding test

Typically, 100 μ L NPM solution in DMF (10 μ M) was added to 1.5 mL lysozyme (2.0 mg/mL, 0.139 mM, in 100 mM NaCl). After the homogeneous mixing, 1.5 mL TCEP (1.0 mM, pH=6.0, in 100 mM NaCl) was added to the mixture. The fluorescence of the reaction was recorded from 350 nm to 430 nm with excitation wavelength at 330 nm (excitation slit: 5.0 nm, and emission slit: 5.0 nm; voltage 700). The disulfide bond of lysozyme can be reduced by TCEP, and the resulting free thiol groups selectively react with the maleimide group of NPM, producing a fluorescent adduct with a high extinction coefficient. The emission intensity at 380 nm was recorded against the incubation time.

Thioflavin T (ThT) staining

The β -sheet sensitive fluorescence dye ThT was used to investigate the β -sheet formation dynamics in bulk solution.^{2,3} Typically, 100 μ L ThT aqueous solution (10 μ M) was added to 1.5 mL lysozyme (2.0 mg/mL, 0.139 mM, in 100 mM NaCl). After the homogeneous mixing, 1.5 mL TCEP (1.0 mM, pH=6.0, in 100 mM NaCl) was added to the mixture. The fluorescence spectrum of the mixture was recorded from 450 nm to 600 nm with excitation wavelength at 440 nm (excitation slit: 5.0 nm, and emission slit: 5.0 nm; voltage 700). The emission intensity at 484 nm was recorded against the incubation time.

1-anilinoanthracene 8-sulfonate (ANS) binding assay

The fluorescence dye ANS was used to investigate the hydrophobic aggregation in bulk solution. Typically, 100 μ L ANS aqueous solution (10 μ M) was added to 1.5 mL lysozyme (2.0 mg/mL, 0.139 mM, in 100 mM NaCl). After the homogeneous mixing, and then 1.5 mL TCEP (1.0 mM, pH=6.0, in 100 mM NaCl) was added into the mixture. The fluorescence spectrum of the mixture was recorded from 390 nm to 550 nm with excitation wavelength at 355 nm (excitation slit: 5.0 nm, and emission slit: 5.0 nm; voltage 400). The emission intensity at 470 nm was recorded against the incubation time.

Asymmetric flow field-flow fractionation coupled with multi angle laser light scattering (AF4-MALLS) analysis

Sample for AF4-MALLS analysis was prepared by mixing equal volume of the aqueous solutions of lysozyme (2.0 mg/mL, in the eluent of 100 mM NaCl) and TCEP (1.0 mM, pH=6.0, in 100 mM NaCl). The first measurement was carried out at 8 min after mixing and filtering the solutions, 40 consecutive runs were performed with a measurement time of 43 min for each run, and the total monitoring time is up to 1728 min (28.8 hrs). The control solution of lysozyme (1.0 mg/mL) in 100 mM NaCl without the addition of TCEP was also measured at the same condition and the resulting $M_w = 14300$ g/mol. No aggregate has been detected after storing the native lysozyme solution at room temperature for days. More details of the experimental procedure can be found elsewhere.⁴

Small angle X-ray scattering (SAXS) analysis

The SAXS measurements of native and unfolded lysozyme solution was performed on a SAXSess mc2 (Anton-Paar, Austria), with Cu-K α , $\lambda = 0.154$ nm and equipped with a CCD detector from

Roper Scientific (pixel size 43 μm), the scattering vector range from 0.05-30 nm^{-1} . The sample to detector distance is 2.5 m. The data collection time is 40 min for each measurement. Lysozyme (10 mg/mL) was mixed with TCEP (10 mM $\text{pH}=6.0$) solution in equal volume for 10 min before testing.

Grazing-incidence small-angle X-ray scattering (GISAXS) analysis

The Janus film was prepared at the air-water interface of the equivoluminal mixture of lysozyme (2.0 mg/mL in 250 mM NaCl) and TCEP (0.5 mM , pH 8.0 in 250 mM NaCl). Typically, 0.5 mL of the freshly prepared reaction solution was dropped on a coverslip (2 $\text{cm}\times 2$ cm) as substrate and incubated in a humid environment for 24 hrs at room temperature. The newly formed Janus film at the air-water interface was floating into MilliQ water, and the free-floating film was obtained at AWI. The free-floating film was collected on a silicon wafer (2 $\text{cm}\times 2$ cm) for more than ten layers for GIWAXS measurement and dried the film with nitrogen whenever there were collected. The GISAXS measurements of Janus nanofilm were performed at beamline BL16B1 at Shanghai Synchrotron Radiation Facility (SSRF). The X-ray wavelength was 0.124 nm , with 10 keV photon energy. A Pilatus 2M detector (1475 \times 1679 pixels) was used for 2D data collection. The sample to detector distance was calibrated with rat tail collagen, which is 1910 mm . The pixel size of the detector is 172 \times 172 μm , and the q -resolution is 4.56 $\times 10^{-3}$ nm^{-1} pixel $^{-1}$. The protein nanofilm was measured on Si substance with the incident angle of 0.2 $^\circ$. The obtained 2D GISAXS images were plotted and transformed into 1D data by Fit 2D software.

Grazing-incidence wide-angle X-ray scattering (GIWAXS) analysis

The Janus nanofilm was floating at the air-water interface, and 10 layers of the film were loaded onto the silicon wafer, then dried with nitrogen before testing. The GIWAXS measurements of Janus nanofilm were performed at beamline BL14B1 at Shanghai Synchrotron Radiation Facility (SSRF). The X-ray wavelength was 0.124 nm , with 10 keV photon energy. A Rayonix mx 225 detector (3027 \times 3027 pixels) was used for 2D data collection. The sample to detector distance was calibrated with LaB6, which is 36 mm . The pixel size of the detector is 73 \times 73 μm , and the q -resolution is 1.025 $\times 10^{-2}$ nm^{-1} pixel $^{-1}$. A 10-layer Janus nanofilm sample on a silicon wafer was measured with an incident angle of 1.0 $^\circ$. The obtained 2D GIWAXS images were plotted and transformed into 1D data by Fit 2D software for further analysis.

Matrix-assisted laser desorption ionization time-of-flight mass spectrometry (MALDI-TOF) analysis

MALDI-TOF spectra were performed on a Microflex (Bruker) in LP_12KDa mode. Sinapic acid (20 mg/mL dissolved in acetonitrile/ H_2O =1/1 and 0.1% trifluoroacetic acid) was used as the matrix. For sample preparation, dilute protein solution (0.1 mg/mL) was equal volume mixing with matrix solution. After intensive mixing with a pipette, a 5 μL mixed solution was dropped on the stainless-steel sample plate and dried at r.t. before measurement. The data is collected with 80% of laser intensity, and the m/z range from 1500-25000 was recorded. Sample solution preparation: traditional lysozyme fibril solution was prepared according to the previous report method.⁵ Typically, lysozyme (20 mg/mL) was dissolved in dialysis water, and the solution pH was adjusted to 2 with hydrochloric acid and kept at 70 $^\circ\text{C}$ for 7 days before measurement. R-Lyz solution was prepared with equal volume mixing of lysozyme (2.0 mg/mL) and TCEP (1.0 mM , $\text{pH}=6.0$, in 100 mM NaCl), and the solution was kept at r.t. for 7 days before measurement.

Time-of-flight secondary ion mass spectrometry (TOF-SIMS) analysis

TOF-SIMS samples were prepared in the following procedure. The typical procedure prepared the Janus nanofilm at the air-water interface (equivoluminal mixture of lysozyme, 2.0 mg/mL in 250 mM NaCl and TCEP 0.5 mM, pH 8.0 in 250 mM NaCl, 24 hrs of incubation). The Janus nanofilm was then free-floating on the surface of MilliQ water. Then silicon wafer (cleaned with piranha solution) was used as the substrate to support both sides of the film and dried with nitrogen before analysis. The measurement was carried out on a TOF.SIMS-5 instrument (IONTOF, Germany). Bi-liquid metal was used as an ion source, and the electric current was set at 1 pA. Five points were collected for each sample and 20 times scanned for each point. The peaks in each spectrum were normalized to the sum of the selected intensities to correct for variations in the total secondary ion yields between different spectra. Principal Component Analysis (PCA) of the positively loaded fragments were performed on an Origin-based PCA application with the contact-air side as reference spectra. The theory of which is described in previous research.⁶ After PCA analysis, the hydrophobic, hydrophilic, and neutral residues were marked with red, blue, and grey points, respectively. Residue hydrophobic/hydrophilic scores at pH 7 were counted according to Monera et al.⁶

Lysozyme expression and NMR backbone assignment

The lysozyme gene was cloned into a pET-32 Ek/LIC vector and transformed into Shuffle *E. coli* to produce thioredoxin-fused recombinant protein. Bacterial cultures were incubated at 18°C in M9 medium for isotopic labeling, using U-¹⁵NH₄Cl and U-¹³C₆ glucose, and induced by 1 mM IPTG at OD₆₀₀ of ~ 0.6. After shaking at 18°C for 16-18 h, the cells were harvested by centrifugation at 5,000 rpm for 10 min at 4°C and resuspended in 30 mL binding buffer (50 mM NaH₂PO₄, pH 8.0, 300 mM NaCl and 10 mM imidazole). After first round of purification using Ni-NTA agarose resin, the sample was dialyzed into a buffer containing 20 mM Tris-HCl, 50 mM NaCl, 2 mM CaCl₂ (pH 8.0) to remove the Trx-Tag by enterokinase (NEB, Cat#P8070S) at 25°C for 16 hours. The sample was then subjected to another immobilized metal affinity chromatography and size exclusion chromatography for further purification. The overall yield for the untagged lysozyme was around 2 mg per 10 liters. The triple resonance experiments were performed in a buffer containing 500 mM NaCl, 50 mM KH₂PO₄ at pH 7.4. NMR spectra were collected at 300 K from Bruker 600 MHz (Avance III) and Bruker 800 MHz (Avance NEO) spectrometers equipped with cryo-probes. Spectral assignments were completed using our in-house, semi-automated assignment algorithms and standard triple-resonance assignment methodology. The titration experiments were performed using ¹⁵N-labelled lysozyme to measure the immediate effect of 25 mM TCEP on protein folding and unlabeled lysozyme measured at natural abundance otherwise. The chemical shift perturbations (CSPs) were calculated using equation $CSP = \sqrt{(\Delta\delta H_N)^2 + (0.1\Delta\delta N_H)^2}$. ¹H-¹⁵N HSQC, HNCACB, CBCA(CO)NH, HN(CA)CO, HNCO experiments were acquired for backbone assignments. For chemical shift residues that are unassigned due to significant chemical shift changes: 5Arg, 6Cys, 19Asn, 24Ser, 25Leu, 45Arg, 52Asp, 126Gly, 127Cys, 128Arg, 129Leu. The spectra were processed using NMRPipe⁷ and analyzed by NMRView.⁸

Transmission electron microscope (TEM) measurement

The following procedure prepared TEM samples for R-Lyz monomer and oligomer. 20 µL freshly prepared R-Lyz solution (equivoluminal mixture of lysozyme, 2.0 mg/mL in 100 mM NaCl and TCEP 1 mM, pH 6.0 in 100 mM NaCl) was dropped onto a clean copper grid covered by amorphous

carbon film. After 5 mins of incubation, the excessive solution was removed by filter paper. The obtained copper grid was then immersed in MilliQ water to remove soluble ions. After removing water with filter paper, 20 μ L of phosphotungstic acid aqueous solutions (2% wt., pH=7, adjusted by 1 mM NaOH aqueous solution) was dropped onto the copper grid for 10 min at rt. The excessive phosphotungstic acid aqueous solution was removed with filter paper, and the grid was dried at r.t. before measurement.

Quartz crystal microbalance (QCM-D) analysis

The Au-coated QCM-D chip was cleaned with a 5:1:1 mixture of MilliQ water, ammonia (25%), and hydrogen peroxide (30%) to 75 °C for 5 mins. Rinse with MilliQ water and dry with nitrogen gas before use. The pipe system was cleaned with 2% SDS solution for 1 h and washed with MilliQ water to keep the resonance signal balance. For QCM-D analysis, protein solution, including native lysozyme (1.0 mg/mL), traditional amyloid fibrils solution (1.0 mg/mL), and R-Lyz solution (equivoluminal mixture of lysozyme, 2.0 mg/mL and TCEP 10 mM, pH 6.0) were injected onto the Au-coated microchip. The frequency and dissipation signal were recorded accordingly. The flow rate was set as 200 μ L/min. All experiments were carried out with a standard Q-Sense flow module (QFM 401) at 25 ± 0.02 °C. The frequency and dissipation singles of 3rd, 5th, 7th, 9th, and 11th were used for data fitting. The surface absorbance capacity was calculated by QsenseDfind software with the Smart method based on 5th frequency data.

Surface plasmon resonance (SPR) analysis

Protein solution, including native lysozyme, traditional amyloid fibril solution, and R-Lyz solution (stack solution: equivoluminal mixture of lysozyme, 2.0 mg/mL and TCEP 10 mM, pH 6.0) with the concentration range from 2.1875 to 70 μ M were injected onto the CM5 sensor chip. The injecting time of all protein solution remains 120 s with the flow rate of 30 μ L/min, followed by the dissociation with MilliQ water for 180s. The chip surface was regenerated between injections with 10 mM NaOH aqueous solution. The response (Ru) signal was recorded accordingly. The kinetic data were analyzed by Biacore T200 Evaluation Software 3.2.1 and fitted with two-state reaction model.

Contact angle tests

The contact angle test of Janus film was measured on a freshly prepared agarose gel (1% wt, 3 cm \times 3 cm) as the substrate to maintain the film at wet conditions. Typically, the free-floating Janus nanofilm on the MilliQ water surface was collected by an agarose gel plate (1% wt, 3 cm \times 3 cm) by pasting out method to expose the contact-water side or by scoop-up method to expose the contact-air side. The excessive water was removed by filter paper. 20 μ L deionized water was ejected onto the film surface, and the contact angle images were collected by an OCA 20 instrument (Dataphysics, Germany). The data was further analyzed by SCA software based on the Youngs equation. Every sample was measured five times to obtain the mean value and error.

Far-UV Circular Dichroism (CD) measurement

The film sample for CD measurement is prepared on quartz slices and cleaned with piranha solution before use. The typical procedure prepared the Janus nanofilm at AWI (equivoluminal mixture of lysozyme, 2.0 mg/mL in 250 mM NaCl and TCEP 0.5 mM, pH 8.0 in 250 mM NaCl, incubated 24

hrs at r.t). The obtained film was free-floating on the air-water interface of MilliQ water, and a precleaned quartz slice was used as the substrate to hold the film. The excessive water was removed by filter paper and dried with nitrogen. For the solution sample, the R-Lyz buffer solution (equivoluminal mixture of lysozyme, 2.0 mg/mL in 100 mM NaCl and TCEP 1.0 mM, pH 6.0 in 100 mM NaCl) was added into a precleaned quartz cuvette with an optical path of 0.02 cm. Transfer the quartz slice or quartz cuvette to the sample room, which optical system is pre-purged with nitrogen for at least 30 mins (N_2 flow rate should be lamp 1.2 L/min; monochromator 3.0 L/min and Sample room, 1.0 L/min). The benchtop CD spectra were collected by a Chirascan spectrophotometer from Applied Photophysics. Every spectrum was taken three times for an average from 180 nm to 260 nm with bandwidth 1 nm, 1 nm step, 0.5 sec/point. The synchrotron radiation circular dichroism (SRCD) spectra were collected on the AU-CD beamline on the ASTRID2 storage ring (ISA, Aarhus University, Denmark). Film samples coated on quartz slices were measured using the hOCD rotation holder (the automated control of multiple angles scanning) with 1 nm step and a dwell time of 2 sec per point in the range of 330-160 nm. A clean quartz window was as a baseline for the subtraction to have the final spectrum. The CD data were further analyzed using Dichroweb (www.cryst.bbk.ac.uk/cdweb) to predict secondary structure construction. According to the literature, the equivalent concentration of the protein film with a thickness of 150 nm was calculated by the absorbance at 205 nm and molar extinction coefficient (ϵ_{205}) at 205 nm.⁹ The ϵ_{205} per residue for R-Lyz equals $4328 \text{ M}^{-1} \text{ cm}^{-1}$, and the equivalent concentration $c(\text{mg/ml})$ is $1.79 \times 10^3 \text{ mg/ml}$. The mean residue weight (MRW) (g/mol) equals to 110.95 Da. Three algorithms were used for comparison, including CONTIN-LL^{10,11}, CDSSTR¹², and SELCON3^{13,14}.

Atomic Force Microscopy (AFM) measurement

Silicon wafer (cleaned with piranha solution) or freshly cleaved mica was used as the substrate. For the oligomer analysis, the freshly cleaved mica was immersed into the R-Lyz reaction solution (equivoluminal mixture of lysozyme, 2.0 mg/mL in 100 mM NaCl and TCEP 1.0 mM, pH 6.0 in 100 mM NaCl) for 5 min and gently washed with deionized water, dried with nitrogen after removing the excess water with filter paper. For Janus film morphology analysis, both sides were coated on a silicon wafer and dried at room temperature before measurement. For the film thickness measurement, the film-coated silicon wafer was scratched by a sharp needle several times rapidly. The cross-section area can be pre-selected by the microscope of the instrument. The measurement was performed on a Dimension ICON instrument from Bruker with a ScanAsyst-Air probe (resonant frequency 70 kHz; spring constant 0.4 N/m) in the smart mood. Images were plotted by NanoScope Analysis 1.8 software.

Liquid phase in-situ Atomic Force Microscopy (AFM) measurement

In-situ AFM analysis was performed on a Cypher VRS by Oxford Instruments. On 3 mm mica discs (SPI-Chem), the native lysozyme solution and R-Lyz reaction solution (equal volume mixture of lysozyme 2.0 mg/mL in 100 mM NaCl, and TCEP 1.0 mM, pH=6.0 in 100 mM NaCl) were poured into the chamber of the liquid holder by injection pump with the speed of 1.2 mL/hr respectively. The measurement is performed with a BL-AC40TS tip (resonance frequency 75 kHz in air, ~25 kHz in water, spring constant 0.08 N/m). The scanning of the mica disc starts before the reaction water reaches the mica surface with a scanning rate of 10 kHz, the movie and snapshots of the protein

aggregation behavior were analyzed and plotted by Cypher VRS AFM software (Asylum research 16.24.225).

Scanning electron microscope (SEM) cross-section analysis

The thickness of the self-assembled nanofilm was analyzed by SEM cross-section image. The film at the air-water interface with different assembly times is collected on a precleaned silicon wafer. The film is dried with nitrogen and washed with MilliQ water. Then film surface is ion sputtered (vacuum at 8×10^{-3} kPa, 40 s) with an Au layer to increase the sample conductivity. Then the sample is placed into liquid nitrogen and broken into two to expose the cross-section area. The freshly prepared cross-section sample was measured using a field emission scanning electron microscope (FE-SEM) at an accelerating voltage of 10 kV. The thickness of the film is measured by ImageJ software based on FE-SEM results.

Ellipsometer analysis

The thickness of the self-assembled nanofilm was characterized by an ALPHA-SE ellipsometer (J.A. WOOLLAM, USA) on silicon substrates. The incident light wavelength was set at 400-800 nm with an incident angle of 45° . The results were fitted with the Cauchy model to obtain the film thickness, refractive index ($n = 1.564$), extinction coefficient ($k=0$), and the thickness of the silicon dioxide oxide layer is 2.5 nm.

X-ray photoelectron spectroscopy (XPS) test

Silicon wafer (cleaned with piranha solution) was used as the substrate for preparing XPS samples. The typical procedure prepared the Janus nanofilm at AWI (equivoluminal mixture of lysozyme, 2.0 mg/mL in 250 mM NaCl and TCEP 0.5 mM, pH 8.0 in 250 mM NaCl, incubate 24 hrs at r.t). The obtained nanofilm was free-floating on the air-water interface of MilliQ water. Then pre-cleaned silicon wafer was used as the substrate to collect both sides of the film and dried with nitrogen before analysis. The sample was analyzed with an ESCALAB Xi+ instrument from Thermo Fisher. The grazing incident angle is 45° . The whole spectrum and high-resolution spectrum of C, N, O, and S elements were acquired. The binding energies were calibrated by setting the C 1s peak at 284.6 eV.

Laser scanning confocal microscopy (LSCM) test

The Janus protein film was prepared by the typical procedure. The film was free-floating on a MilliQ water interface and collected with a glass slice (cleaned with piranha solution). The excessive water was removed by filter paper and dried with nitrogen (Notice: to preserve the boundary of the film for better focus). The obtained sample was immersed into a ThT aqueous solution (10 μ M) for 1.5 hrs and washed with MilliQ water, and dried with nitrogen. The ThT stained glass slice was measured with an FV1200 LSCM from Olympus. The bright-field image and dark-field fluorescent image were obtained by 488 nm laser irradiation.

Surface-enhanced Raman spectroscopy (SERS)

The silver nanoparticles (AgNPs) required for SERS measurement are prepared by literature methods,¹ washed with MilliQ water several times, and centrifuged before use. The particle size of the AgNPs is around 60-100 nm. Typically, the free-floating Janus nanofilm on the MilliQ water

surface was collected by silicon wafer by paste out method to expose the contact-water side or by scoop up method to expose the contact-air side. The excessive water was removed by filter paper and dried with nitrogen before measurement. The freshly prepared AgNPs solution was dropped on the upper layer of the film to perform the Raman test by using a Renishaw inVia reflex confocal Raman spectrometer. A 532 nm laser source was used, the laser intensity was set as 0.1%, and the Raman shift was recorded from 400 cm^{-1} to 4000 cm^{-1} . Before measurement, it must be confirmed that the laser focuses on the protein film surface. Each sample takes five different positions and performs twice for each point. The obtained data were averaged to reduce errors. The spectra of the contact-air and contact-water sides were normalized with the intensity of peaks at the 1396 cm^{-1} regions corresponding to the $C_{\alpha-H}$.

Nanoindentation analysis

The Janus nanofilm obtained by typical methods (equivoluminal mixture of lysozyme, 2.0 mg/mL in 250 mM NaCl and TCEP 0.5 mM, pH 8.0 in 250 mM NaCl, incubated 24 hrs at r.t) was floating at the air-water interface of MilliQ water. The silicon wafer (2 cm \times 2cm) was used as the substrate. The excessive water was removed by filter paper at the corner of the silicon wafer and gently dried with nitrogen to protect the surface morphology. Ten layers of the film were stacked for the nanoindentation test, which is performed on a Hysitron TI 980 Nanoindenter from Bruker. A Berkovich diamond probe (142.3 degrees, 100 nm tip radius, Young's modulus 1140 GPa, Poisson's ratio, 0.07) was used with the pierce depth as 100 nm, interaction time is 16 s. Each sample was tested five times at different positions, and the obtained results were averaged to reduce errors.

Shear test for adhesion strength measurement

The Janus nanofilm was prepared by an equivoluminal mixture of lysozyme (2.0 mg/mL in 250 mM NaCl) and TCEP (0.5 mM, pH 8.0 in 250 mM NaCl) on a coverslip (2 cm \times 4 cm) substrate. After incubation in a humid environment for 24 hrs at r.t, the obtained Janus nanofilm floated onto the air-water interface and was pasted out (contact-air side attached to the glass) or scooped up (contact-water side attached to the glass) from the water with two glass plates (1 cm \times 5 cm with 4 mm circular hole). The two glass plates were stuck face by face and clamped together with a metal clip. The plates were dried at r.t for 24 hrs before the tensile shear test. The tensile shear test was performed by a UTM 2103 mechanical test machine. The capacity of the tension sensor is chosen as 100 N. The tensile test was performed in a vertical direction, and the separation speed was 5 mm/min. The maximum breaking strength was recorded from the stain-stress curve. Each group recorded 10 samples, and the obtained results were averaged to reduce errors.

Swelling testing of Janus nanofilms

The swelling performance of the Janus nanofilms on a silicon wafer was tested by reflectance spectroscopy within the visible light range (400-900 nm) under different humidity conditions. The thickness change of the film can be calculated through the Bragg equation: $2 n_2 d \cos \theta = m \lambda$, where d is the thickness of the film, θ is the angle of incident light, which is perpendicular to the sample surface ($\theta = 0^\circ$, $\cos \theta = 1$), λ is the wavelength of the interfering light, and m denotes an integer ($m = 1, 2, 3, \dots$). The refractive indices of air, the protein film, and silicon are represented as $n_1 = 1$, $n_2 = 1.56$, and $n_3 = 3.8$, respectively.

Young's modulus test from tension machine

The Janus nanofilm was obtained by typical methods, and the film was collected by a hollowed box (1.8 cm × 3.6 cm) for 15-20 layers. The obtained multi-layer Janus nanofilm was dried in air at r.t. The dried multi-layer film (with a thickness of 2-3 μm) was cut into a 2.5 cm × 0.5 mm rectangle clip and fixed with double sticky tape on the square filter paper (0.6 mm × 0.6 mm). The tensile test was performed in a horizontal direction of the sample clip with an IBTC-100S tension machine from CARE company. The film was stretched at a 1 mm/min rate, and the force-distance curve was obtained. The original data was further converted to a strain-stress curve based on the initial sample length. The exact thickness of the multi-layer film was determined by SEM cross-section image.

Replica exchange Molecular dynamic (REMD) simulation

Lysozyme (PDB ID: 1DPX) was treated to reduce 4 disulfate bonds with Gromacs 2019.6 software.¹⁴ The REMD simulation was carried out by Gromacs 2019.6 software with Gromos 53A6 force field under constant temperature, pressure and periodic boundary conditions.¹⁶ A vacuum-water interface is utilized to mimic the air-water interface.¹⁷ Water molecule was used in the SPC model. In the MD simulation process, all hydrogen bonds involved are constrained by the LINCS algorithm,¹⁸ and the integration step is 2 fs. Electrostatic interaction is calculated by (Particle-mesh Ewald) PME method.¹⁹ The cutoff value for non-bonding interactions is set to 10 Å, which is updated every 10 steps. During the REMD simulation process, within the temperature range of 300 K to 420 K, an online server (<http://folding.bmc.uu.se/remd-temperature-generator/>) was used to predict the temperature distribution of each copy, and 66 copies were generated in total. All copies run in parallel, and each copy performs 50 ns REMD simulation for a total of 3.3 μs. The V-rescale²⁰ temperature coupling method is used to control the simulated temperature. First, the steepest descent method is used to minimize the energy of the two systems to eliminate the close contact between the atoms; then, the NVT equilibrium simulation of 100 ps is performed at the temperature of each copy; finally, the 66 copies are respectively performed 50 ns. In the MD simulation of ns, the adjacent temperature copies are exchanged every 300 steps, and the conformation is saved every 20 ps. The free energy change of R-Lyz was calculated by the molecular mechanics Poisson-Boltzmann surface area (MM-PBSA) approach.²¹ The origin-based adjacent-averaging algorithm smoothed the radius of gyration (Rg) and root-mean-square distance (RMSD) data during the simulation time. The simulation results are visualized using Gromacs embedded program and VMD.

Molecular dynamic (MD) simulation

Molecular dynamics simulations were conducted using Gromacs 2019.6 software, and the Gromos 53A6 all-atom force field in conjunction with the SPC water model was employed for the disulfide bond reduced hen egg-white lysozyme (PDB:1DPX). A vacuum-water interface is utilized to mimic the air-water interface.¹⁷ Six lysozymes were randomly placed in a box and filled with water solvent and counter ions. The simulation was running at 333 K. During the MD simulation for 1000 ns, all involved hydrogen bonds were constrained by the LINCS algorithm,¹⁸ and the integration step was set as 2 fs. Electrostatic interactions were calculated using the (Particle-mesh Ewald) PME method¹⁹. The visualization of the simulation results was done using the Gromacs embedded program and VMD. Hydrophobic interaction was analyzed by using YASARA software.²² Hydrogen bonding, Coulomb force and Lennard-Jones (LJ) potential were all calculated based on the analysis module from Gromacs 2019.6 software.

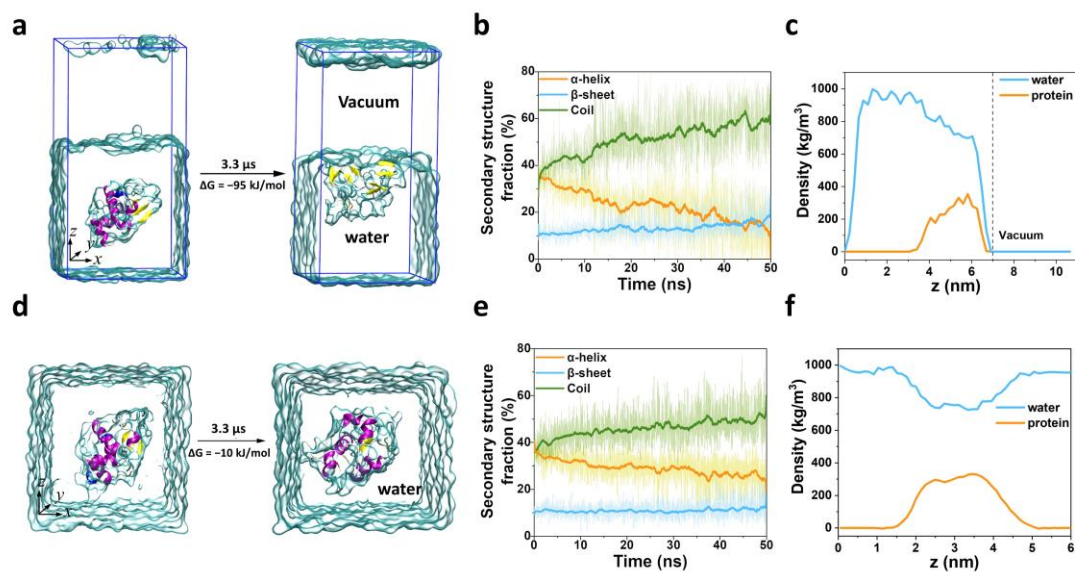


Figure S1. REMD results of R-Lyz at the VWI and in water. Typical configuration of R-Lyz at the VWI (a) and in water (d) from the 310 K replica; Secondary structure fraction of R-Lyz against simulation time at the VWI (b) and in water (e) from 310 K replica; Protein density distribution at the VWI (c) and in water (f).

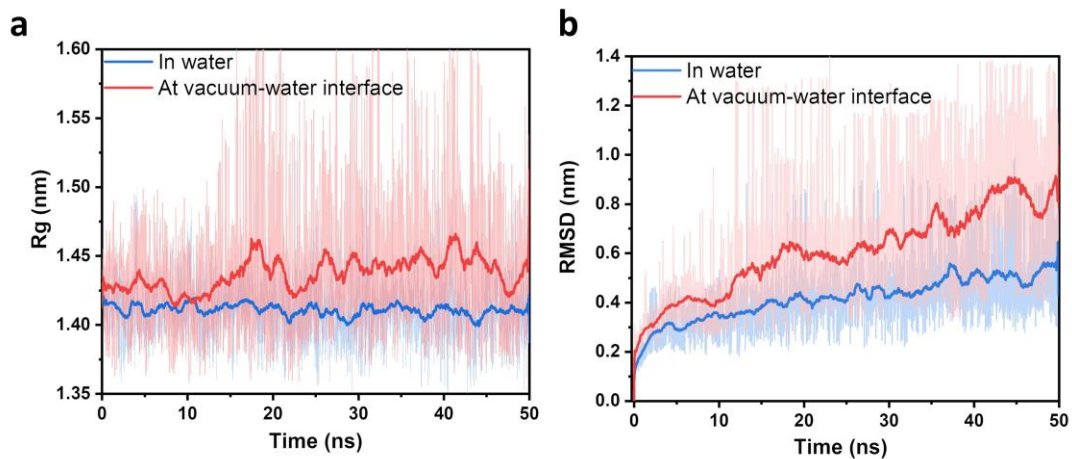


Figure S2. MD simulation results of radius of gyration (Rg) and root-mean-square distance (RMSD). (a) Rg of the R-Lyz from the 310 K replica; (b) The RMSD of the R-Lyz from the 310 K replica.

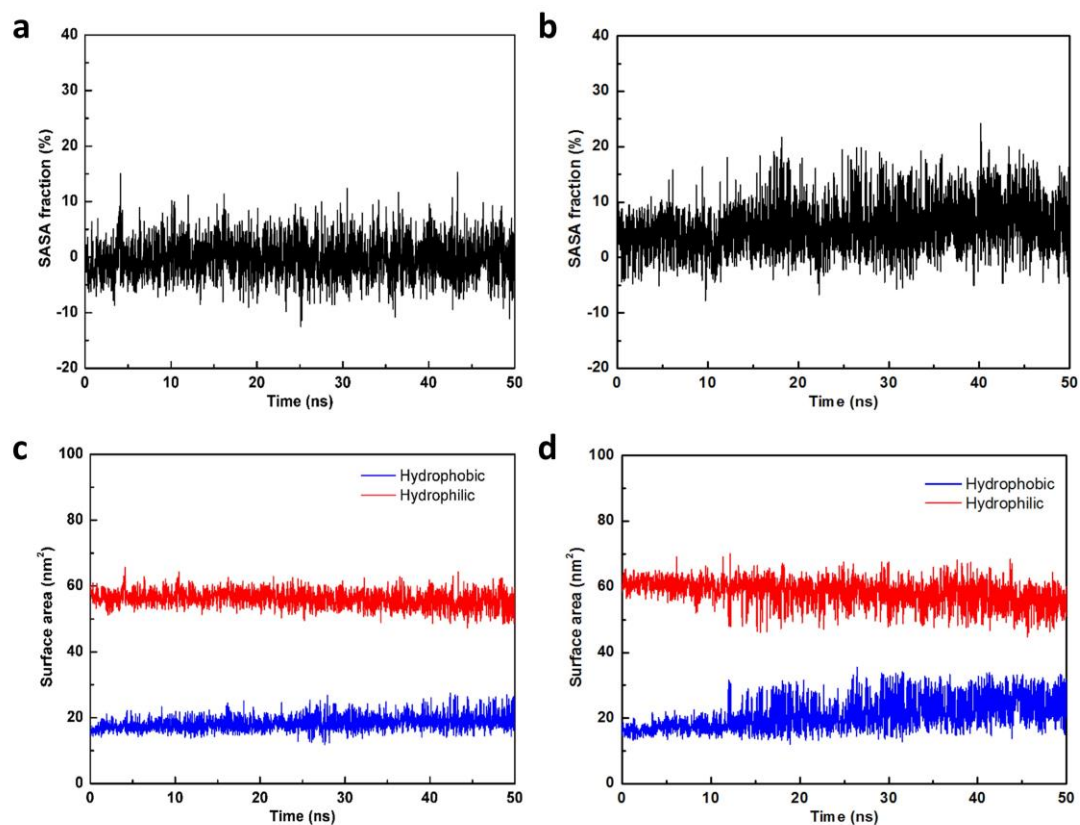


Figure S3. MD simulation results of solvent accessible surface area (SASA). SASA fraction of R-Lyz against simulation time in water (a) and at vacuum-water interface (b). The hydrophobic and hydrophilic surface area of R-Lyz against simulation time in water (c) and at vacuum-water interface (d).

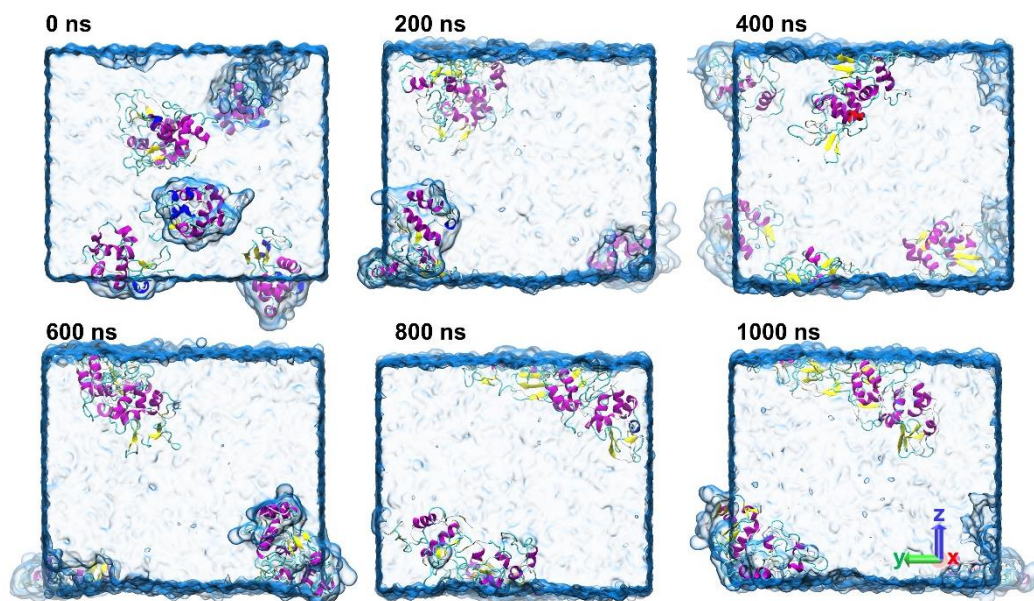


Figure S4. Snapshots of MD simulation. (Every 200 ns from the result of six R-Lyz at vacuum-water interface after 1000 ns).

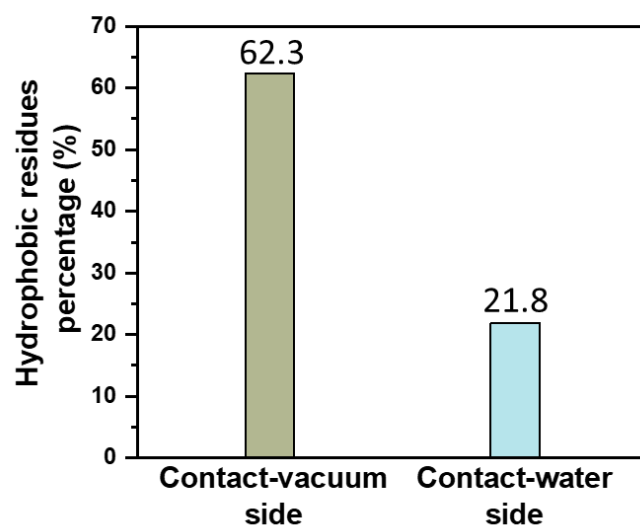


Figure S5. Summarize of MD simulation result. Hydrophobic residues percentage of MD simulation result at contact-vacuum side and contact-water side.

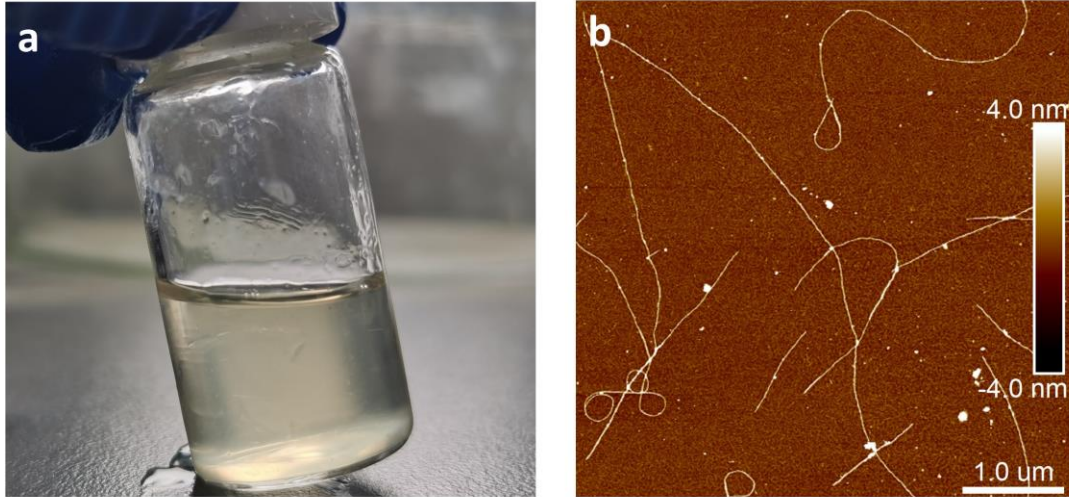


Figure S6. Characterization of traditional amyloid fibril. (a) Digital image and (b) AFM morphology of traditional amyloid fibrils.

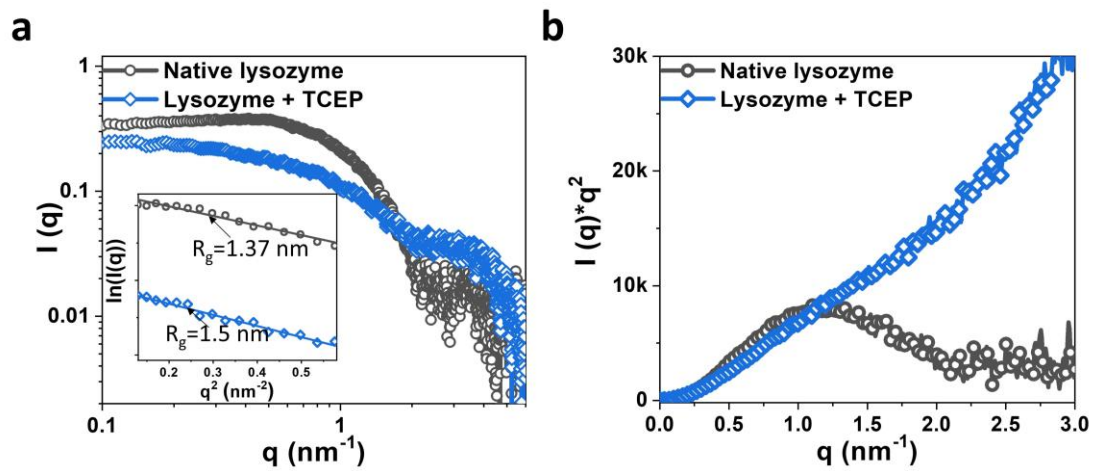


Figure S7. SAXS analysis of native lysozyme and R-Lyz. (a) SAXS data of native lysozyme and R-Lyz solution, inset: corresponding Guinier plot and R_g values; (b) Kratky plot of native lysozyme and R-Lyz.

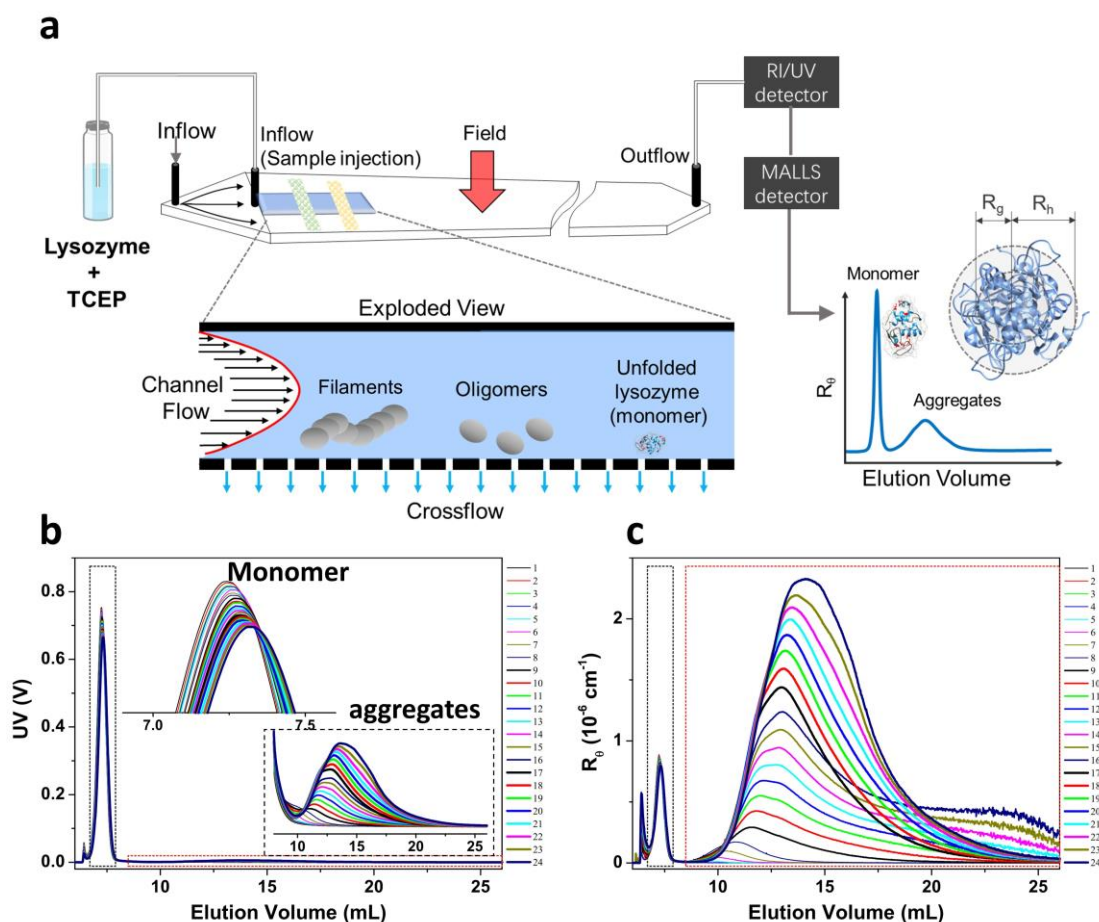


Figure S8. Schematic illustration of asymmetric flow field-flow fractionation (AF4) and the analysis of R-Lyz in bulk solution. (a) Schematic illustration of AF4 measurement of oligomer and curly filaments of lysozyme in bulk solution; (b) UV response and (c) Rayleigh ratio at 90.0° for R-Lyz eluting from the AF4 channel with different cultivation time (line 1-24 represent different runs of measurements, 43 min for each run). Lysozyme monomers elute out at elution volume from 6.7-7.9 mL, and the aggregates elute out at elution volume between 8.5 and 26 mL.

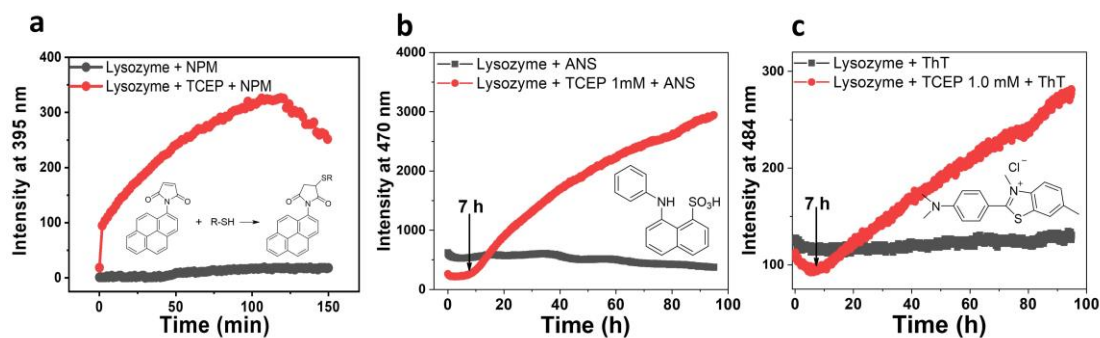


Figure S9. The fluorescence assay results. The fluorescence assay for the equal volume mixtures of lysozyme (2.0 mg/mL, 0.139 mM, in 100 mM NaCl) and tris(2-carboxyethyl) phosphine (TCEP, 1.0 mM, pH=6.0, in 100 mM NaCl): (a) N-(1-pyrenyl) maleimide (NPM) (the fluorescence declining of the mixed solution after 2 hrs is attributed to the aggregation of the protein for the hydrophobic nature of pyrenyl); (b) 8-anilinonaphthalene-1-sulfonic acid (ANS); (c) thioflavin T (ThT). The long lag phase of the ANS and ThT experiment is mainly caused by the relatively stable structure of R-Lyz in the bulk solution compared with AWI. According to the literature,³ ThT is less sensitive with oligomers, which can be the reason for the fluorescence increase being 4 hrs later than the first detection of oligomers (~3 hrs) by AF4. It is worth noting that even a few amyloid-like aggregates formed in bulk solution after 7 hrs of incubation, most of the R-Lyz monomers remain its α -helix-dominated conformation according to CD spectrum (**Figure 2f**).

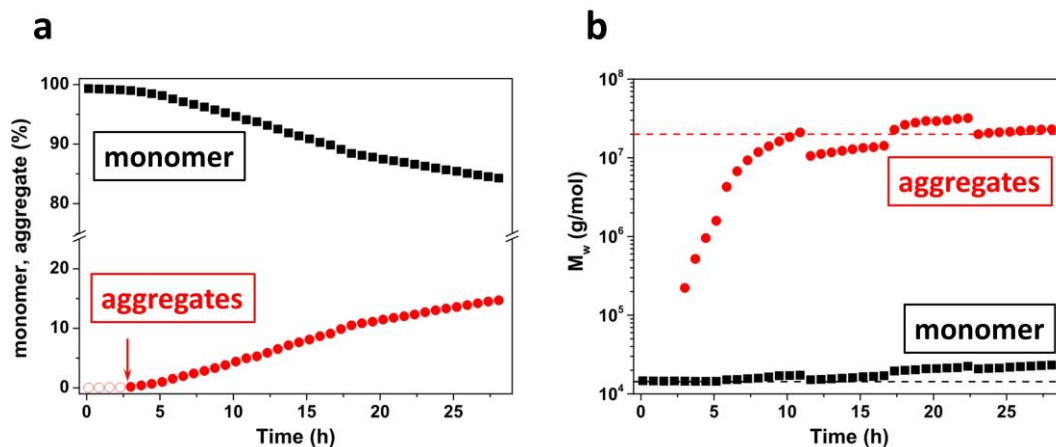


Figure S10. AF4 analysis of R-Lyz in solution. (a) Relative content of monomer and aggregate in bulk solution; (b) Weight average molecular weight M_w of the monomer and aggregates in bulk solution. Note: in the late stage of the cultivation (>15 hrs) of the R-Lyz solution, a small amount of the filaments eluted in a steric mode, leading to the co-elution of small quantities of very large aggregates with the lysozyme monomer. It leads to a deviation of 1st order Berry method and the apparent M_w of the lysozyme monomer increase with time by up to 60%.²³

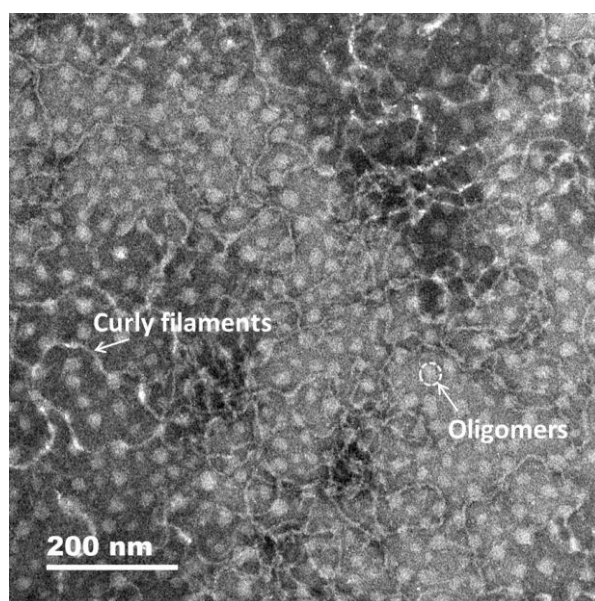


Figure S11. TEM image of oligomers and curly filaments in bulk solution after 24 hrs of incubation (stained with phosphotungstic acid for 10 min before measurement)

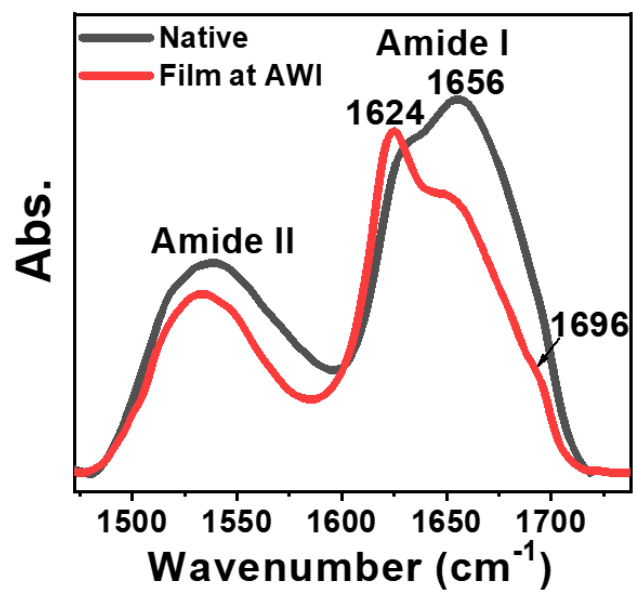


Figure S12. FTIR spectrum (amide I region). Native lysozyme in solution and unfolded protein aggregation (film) at the air-water interface.

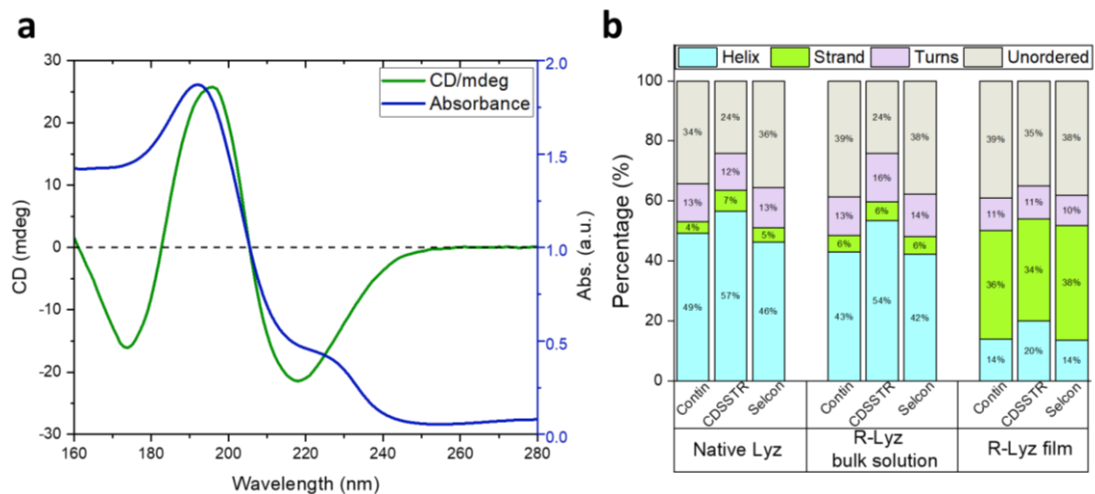


Figure S13. SR-CD and UV-Vis spectrum of R-Lyz nanofilm and their secondary structure calculation. (a) SR-CD spectrum and UV-Vis absorption plot of R-Lyz nanofilm; (b) Calculated secondary structure component of native lysozyme, R-Lyz in bulk solution and R-Lyz nanofilm.

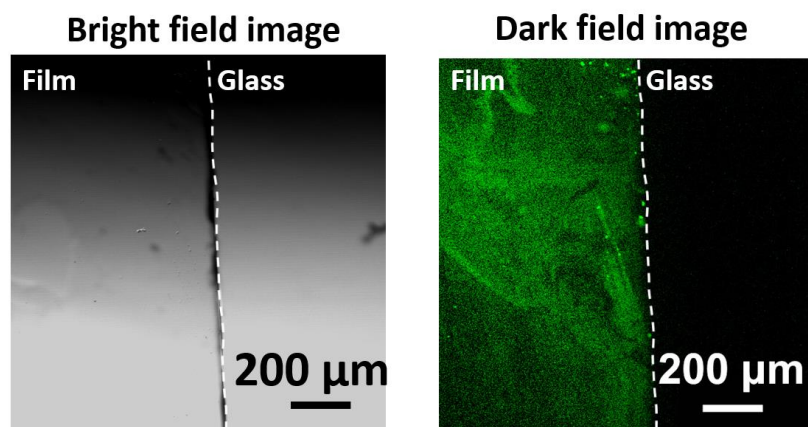


Figure S14. Confocal laser microscopy images of Janus nanofilm. (A) bright field image; (B) dark field image.

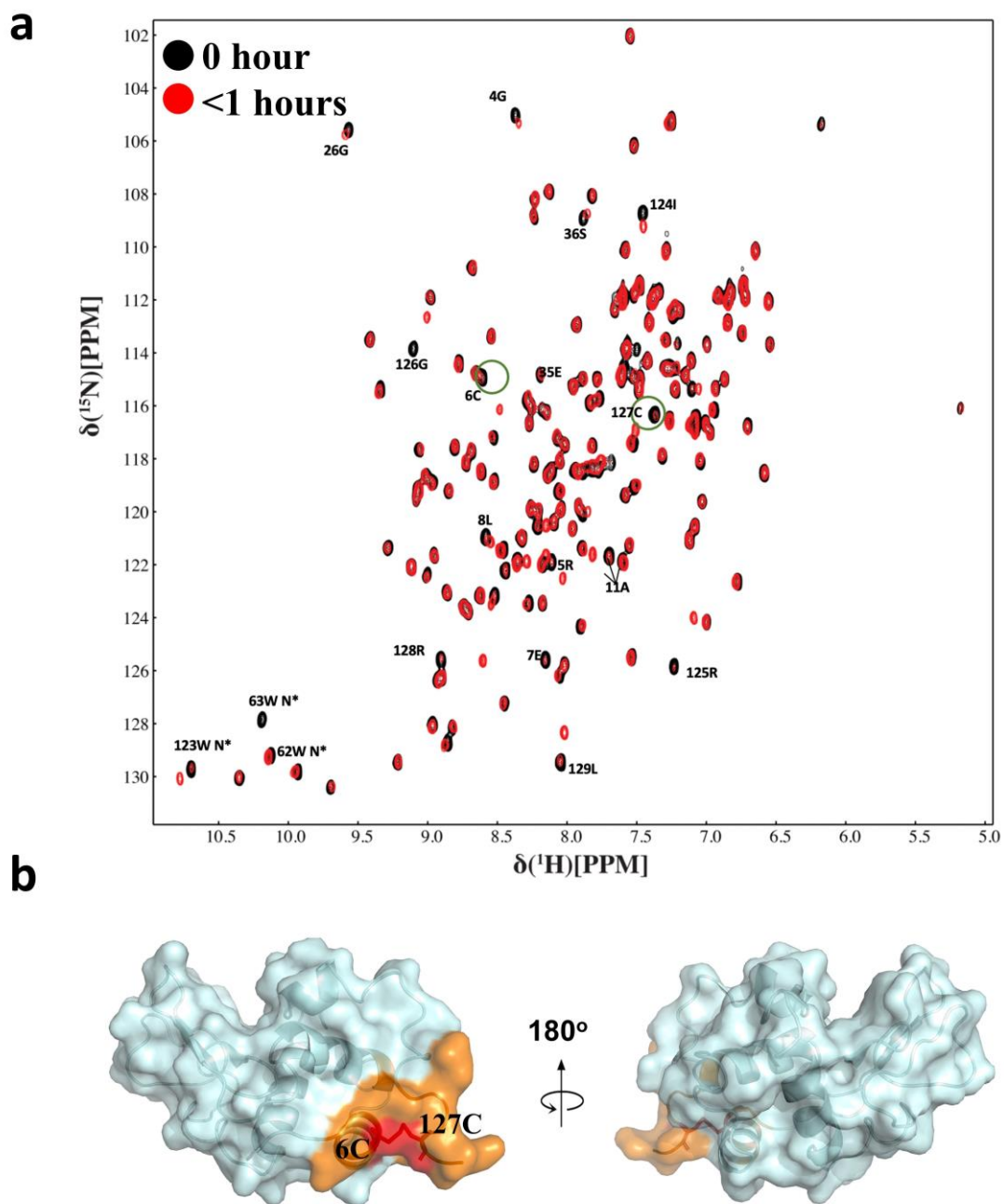


Figure S15. The effect of TCEP on lysozyme structure. (a) The overlay of HSQC spectra of lysozyme before and after adding TCEP. The spectrum was measured immediately after TCEP was added and the peaks experiencing major broadening effect are labelled. (b) The projection of peaks experienced broadening effect on the structure of lysozyme (PDB ID: 1321). The disulfide bond between 6C and 127C was disrupted first prior to other disulfide bridges.

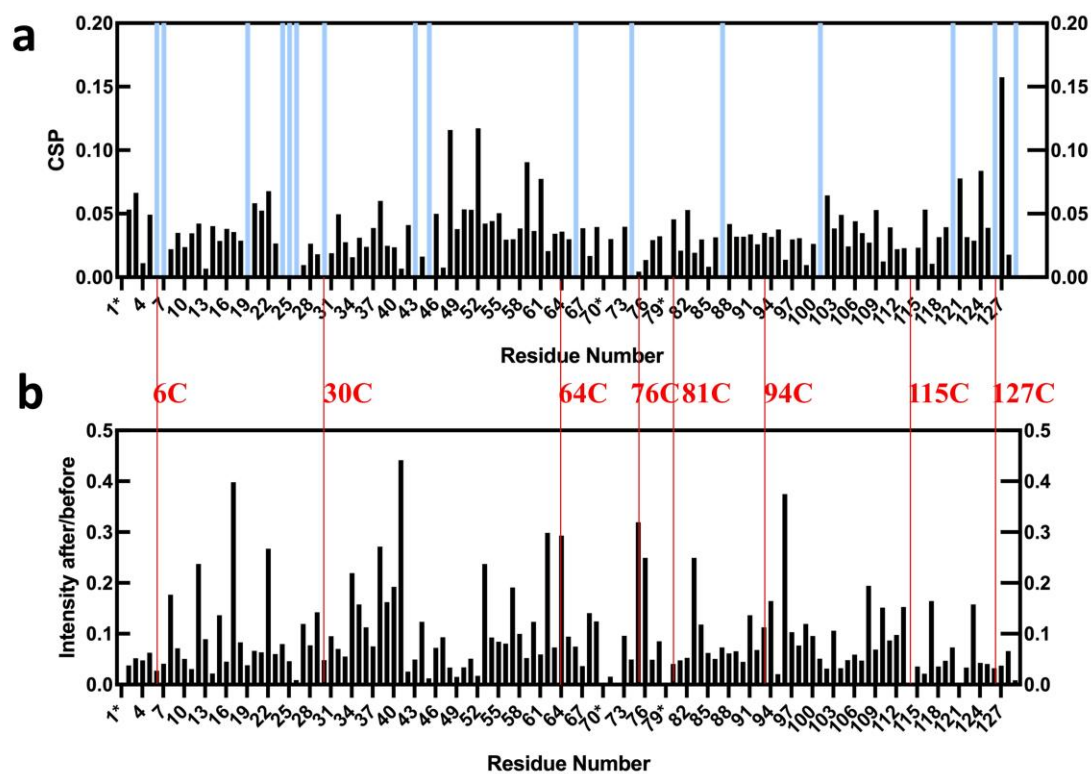


Figure S16. The effect of TCEP on chemical shift perturbations (CPS) and peak intensity of lysozyme. (a) The CSP between the spectra before and after adding TCEP for 3 hours was plotted against residue number. (Major chemical shift perturbations and peak broadening effects were observed, and the blue column indicates the biggest chemical shift in the spectra) (b) The peak intensity difference between the spectra before and after adding TCEP for 3 hours was plotted against residue number.

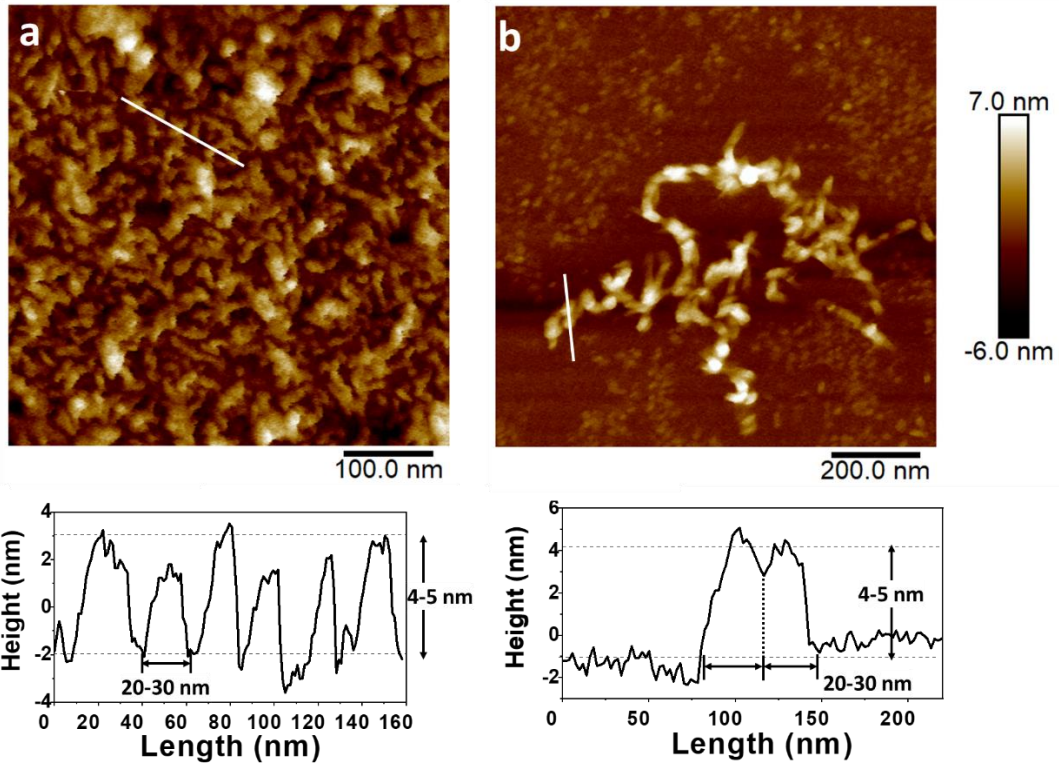


Figure S17. AFM images and cross-section profile of plate-like oligomers in other protein system. (a) $A\beta_{1-42}$ (1 mg/mL in 100mM NaCl on after incubate 10s on freshly cleaved mica) and (b) *E. coli* adhesion layer after ultrasonic treatment for 2 min in MilliQ water.

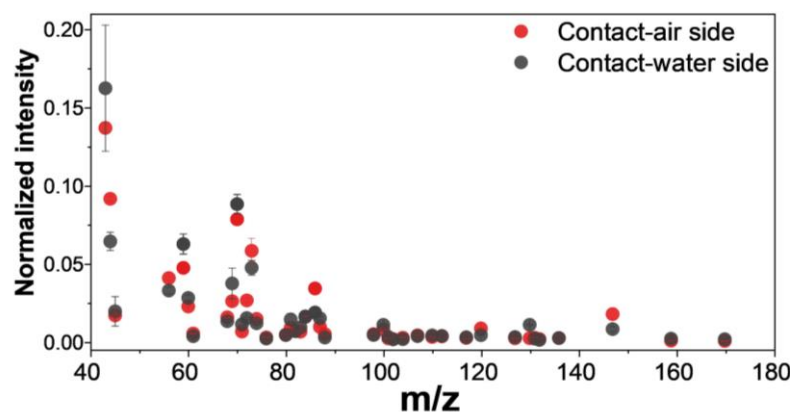


Figure S18. TOF-SIMS result of contact-air side and contact-water side of the film at AWI.

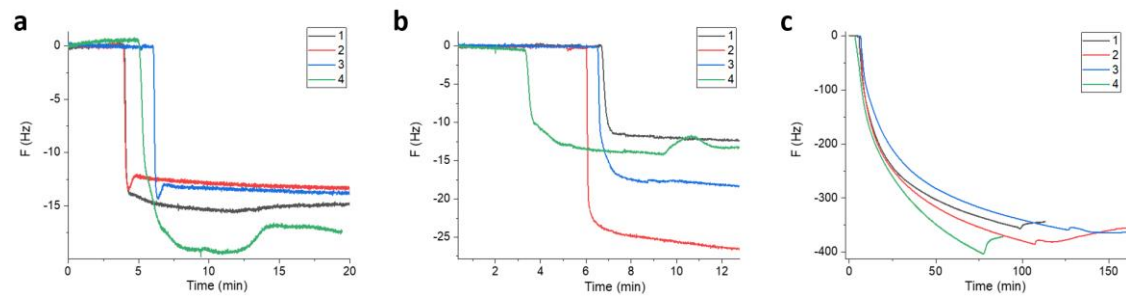


Figure S19. QCM-D results. (a) Native lysozyme (1.0 mg/mL); (b) Traditional lysozyme amyloid fibrils (1.0 mg/mL); (c) R-Lyz solution (lysozyme concentration at 1.0 mg/mL).

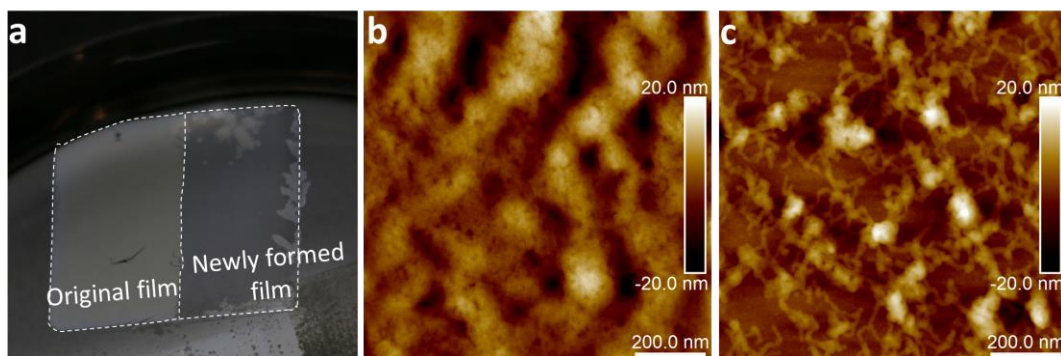


Figure S20. Evidence of interfacial activity of filaments fibrils. (a) Photograph of film at AWI after removing the original film at 30min; (b) AFM image of original film and (c) newly formed film after removing the original film at 60 min.

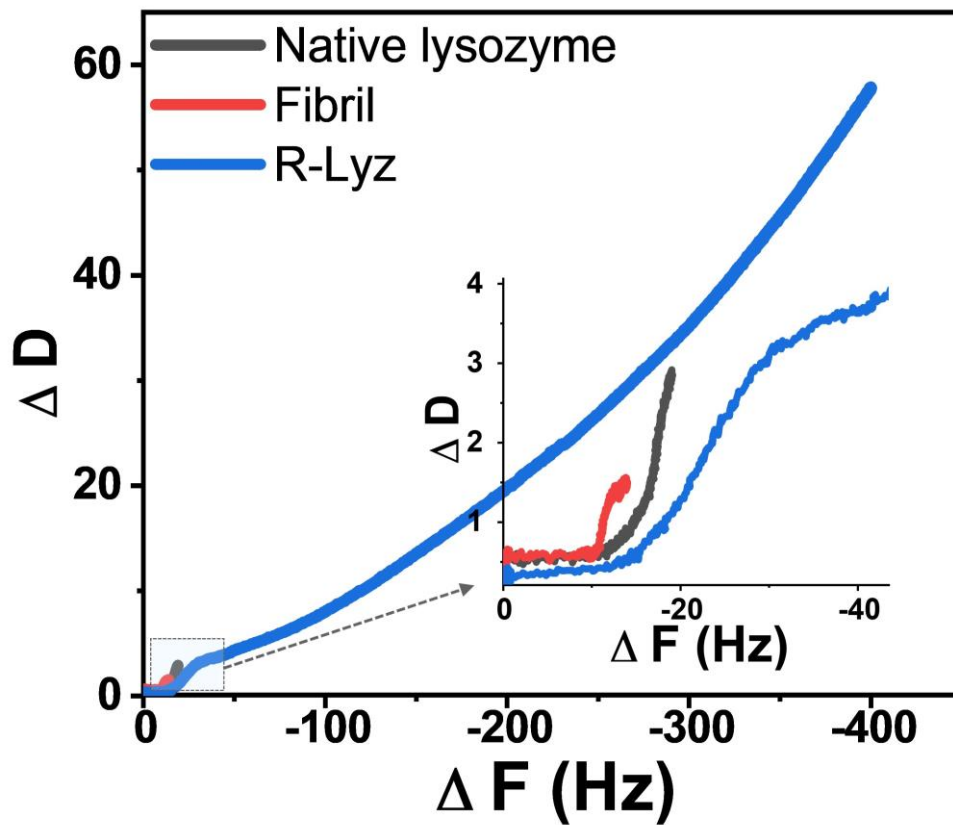


Figure S21. Two stage aggregation of R-Lyz on QCM chip. $\Delta D/\Delta F$ curve of QCM-D analysis of native lysozyme, traditional lysozyme amyloid fibrils and R-Lyz solution on Au sensor. The changing of the slope of $\Delta D/\Delta F$ curve of R-Lyz implying a relatively soft/viscoelasticity layer formed at the initial stage of the assembly (< -30 Hz), followed by the formation of a relatively rigid layer (> -30 Hz).

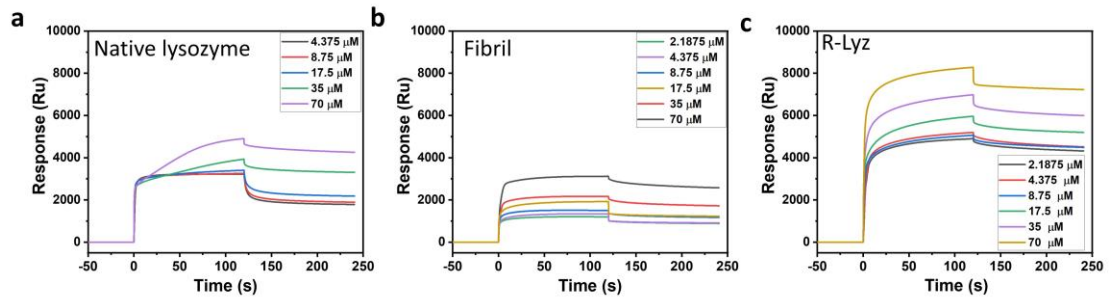


Figure S22. Two stage aggregation of R-Lyz on SPR chip. SPR results of (a) native lysozyme, (b) traditional lysozyme amyloid fibrils and (C) R-Lyz solution with the concentration range from 2.1875 μM to 70 μM on CM5 sensor.

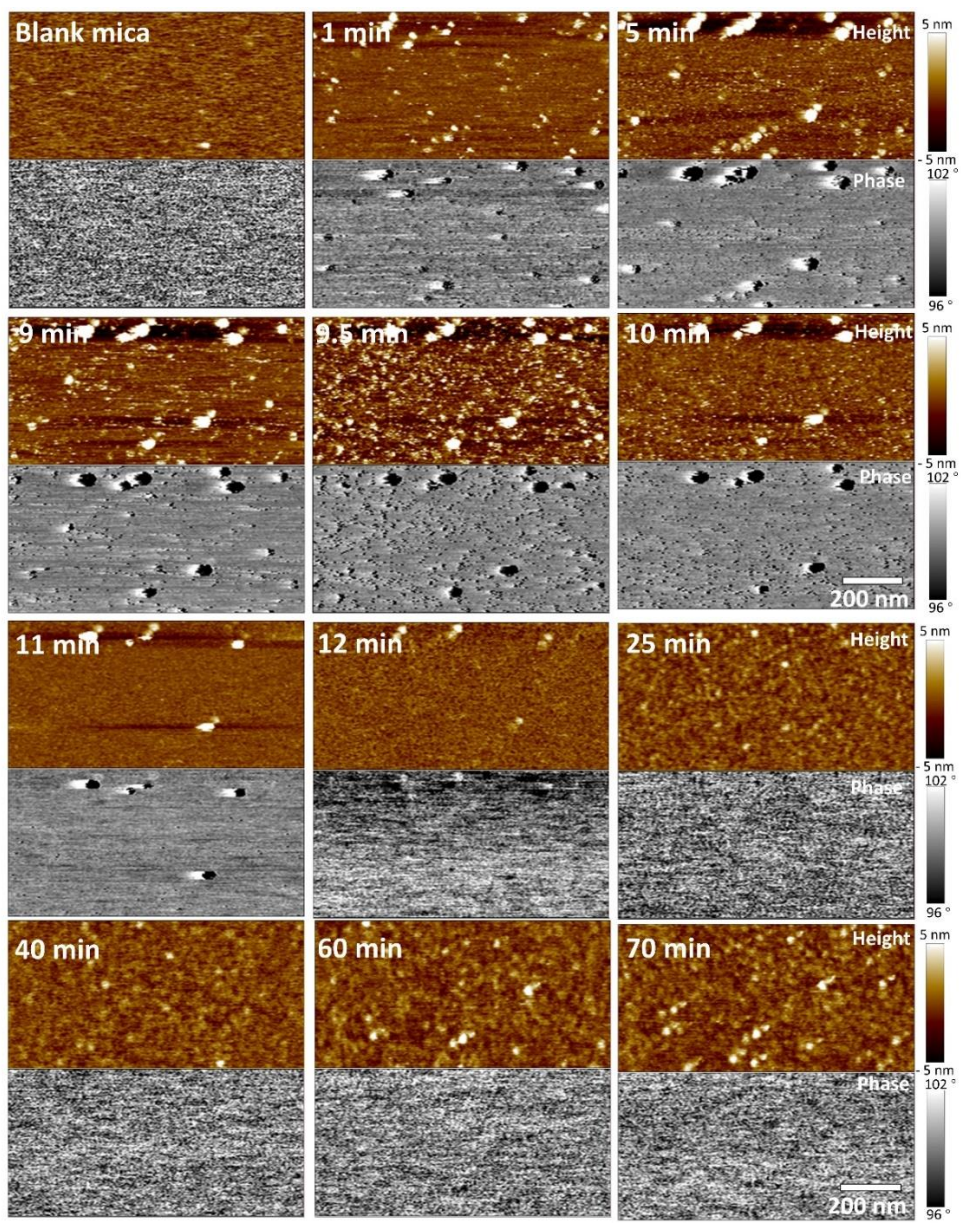


Figure S23. Snapshots of in-situ AFM movie of R-Lyz solution on mica surface with different time.

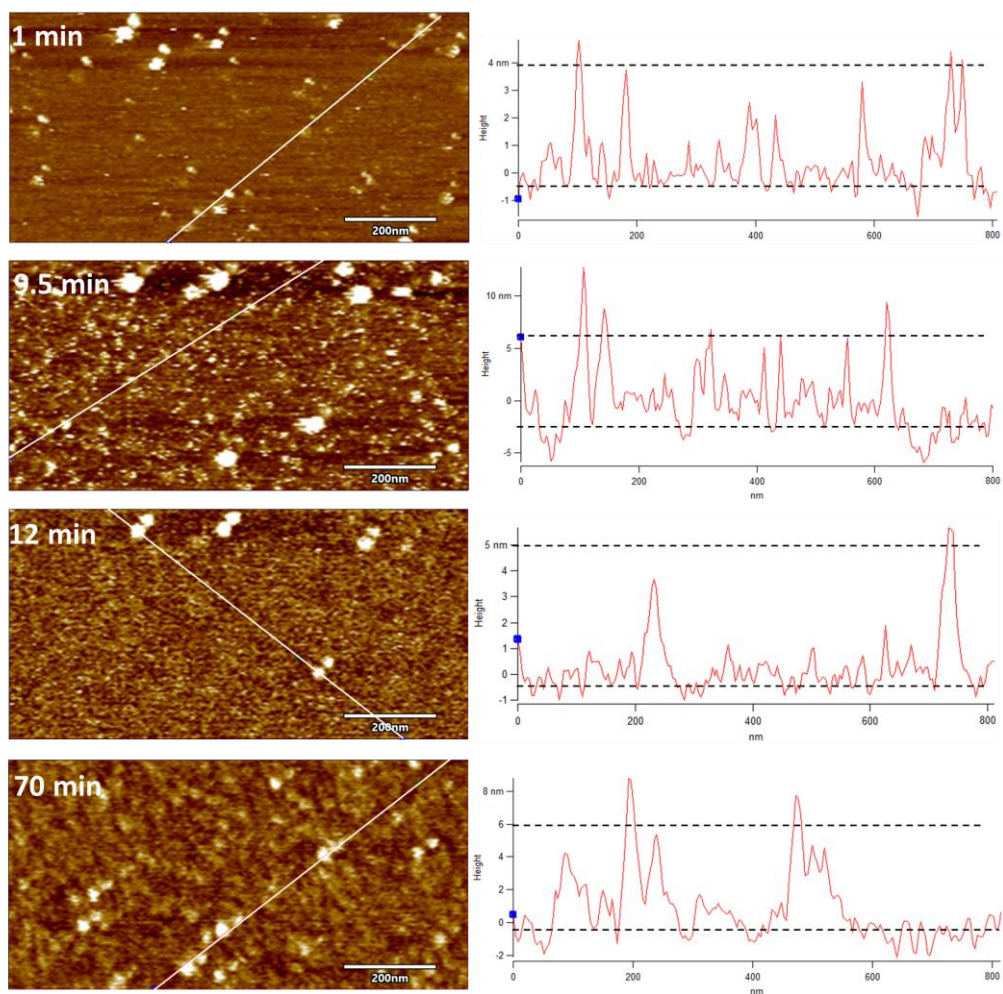


Figure S24. Snapshots and cross-section profile of in-situ AFM movie of R-Lyz solution on mica surface with different time.

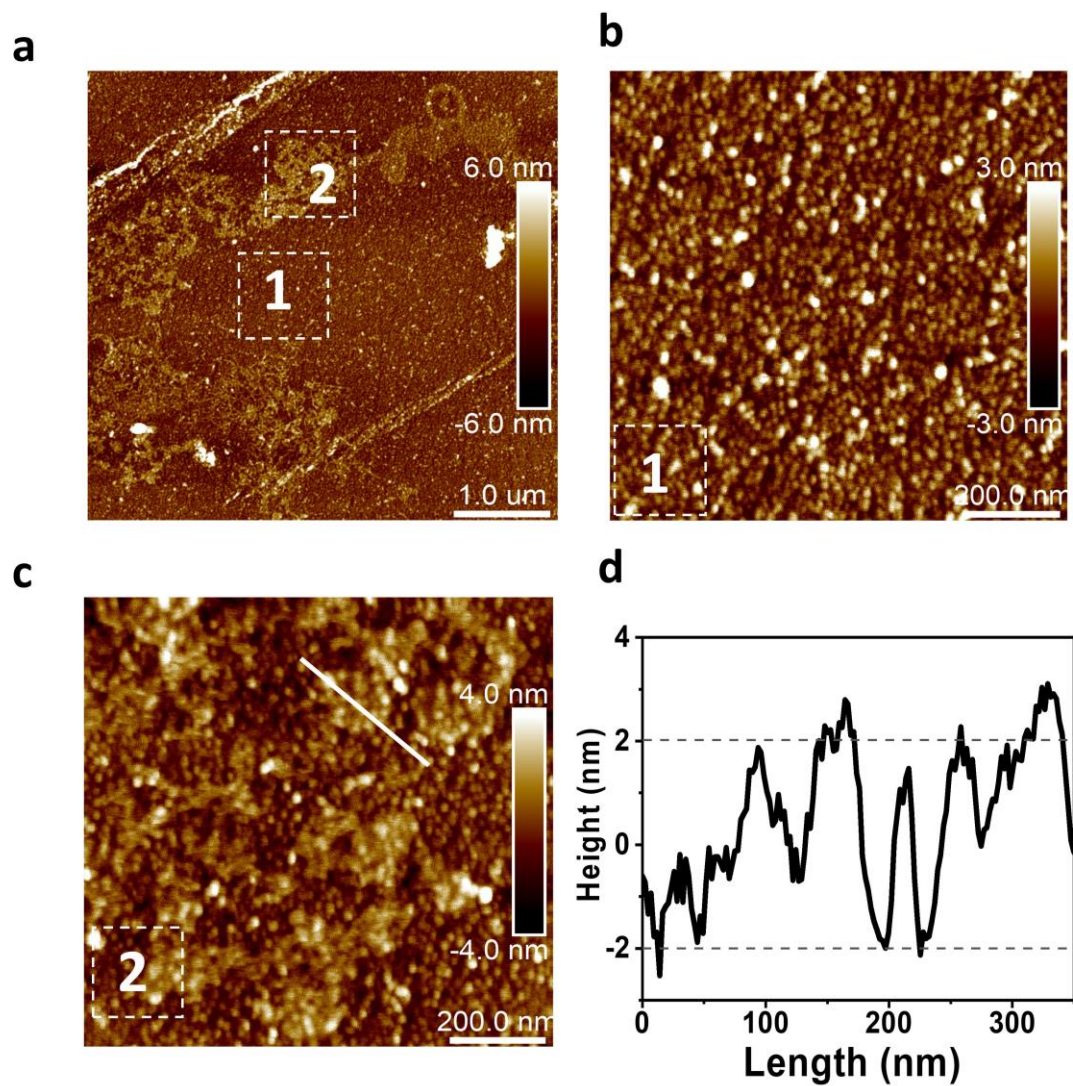


Figure S25. Characterization of R-Lyz film at AWI. (a) AFM image of aggregation morphology of unfolded proteins at AWI (contact water side); (b) Magnified area 1; (c) Magnified area 2; (d) Cross-section analysis of the white line in area 2. (Sample was collected at the AWI of the reaction solution of lysozyme, 2.0 mg/mL with an equal volume of TCEP, 10 mM, pH=6 after 10 mins, contact-water side faces up)

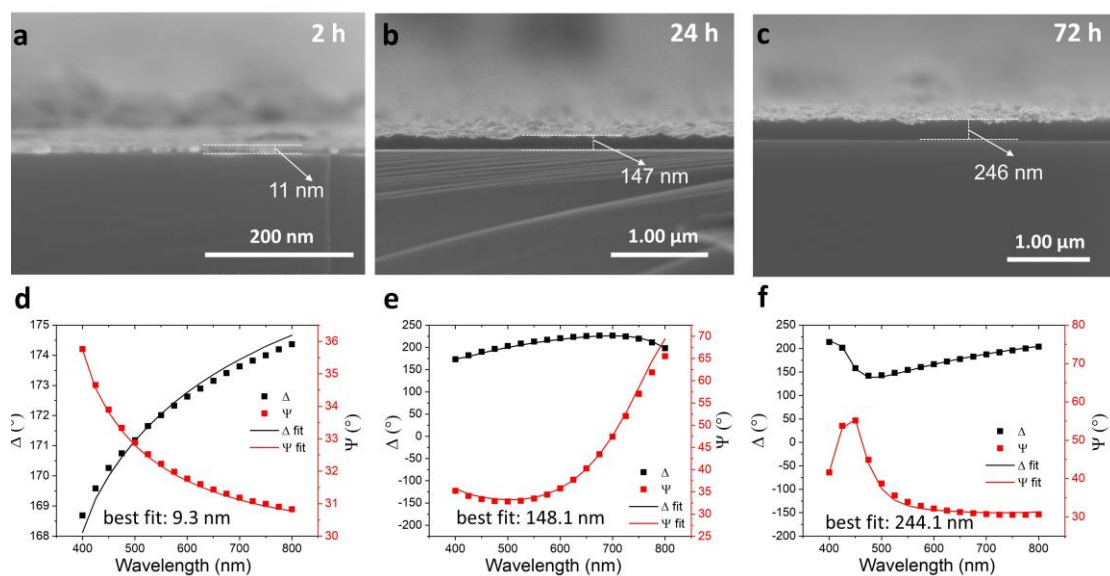
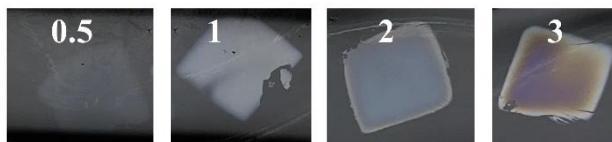


Figure S26. Examples of film thickness analysis by SEM and ellipsometer (Eli). Cross-section SEM image of self-assembled R-Lyz nanofilm after incubation of (a) 2h; (b) 24h; (c) 72h. Fitting of Eli results of R-Lyz nanofilm after incubation of (d) 2h; (e) 24h; (f) 72h.

Score of the film



TECP solution	NaCl conc. mM	Time (h)				
		5.5	10	24	40	48
pH 6	0	×	×	×	×	×
	125	×	×	×	0.5	0.5
	250	×	×	0.5	0.5	0.5
	500	×	0.5	0.5	0.5	0.5
	1000	×	×	×	×	×
pH 7	0	×	×	×	×	×
	125	×	×	×	1	1
	250	×	×	1	2	2
	500	×	1	1	2	2
	1000	×	0.5	1	1	1
pH 8	0	×	0.5	0.5	0.5	0.5
	125	1	1	1	1	1
	250	1	2	2	2	1
	500	1	1	2	3	2
	1000	0.5	1	2	3	3
pH 9	0	×	0.5	0.5	0.5	0.5
	125	1	1	1	1	1
	250	2	2	2	2	2
	500	0.5	2	2	3	3
	1000	0.5	1	1.5	3	3

Figure S27. Strength evaluation of Janus nanofilm under different formation conditions. The visualization appearance of Janus nanofilms obtained from different pHs of the reducing agent, system salt concentration, and reaction time (lysozyme concentration was fixed as 2.0 mg/mL, and TCEP concentration was fixed as 0.5 mM).

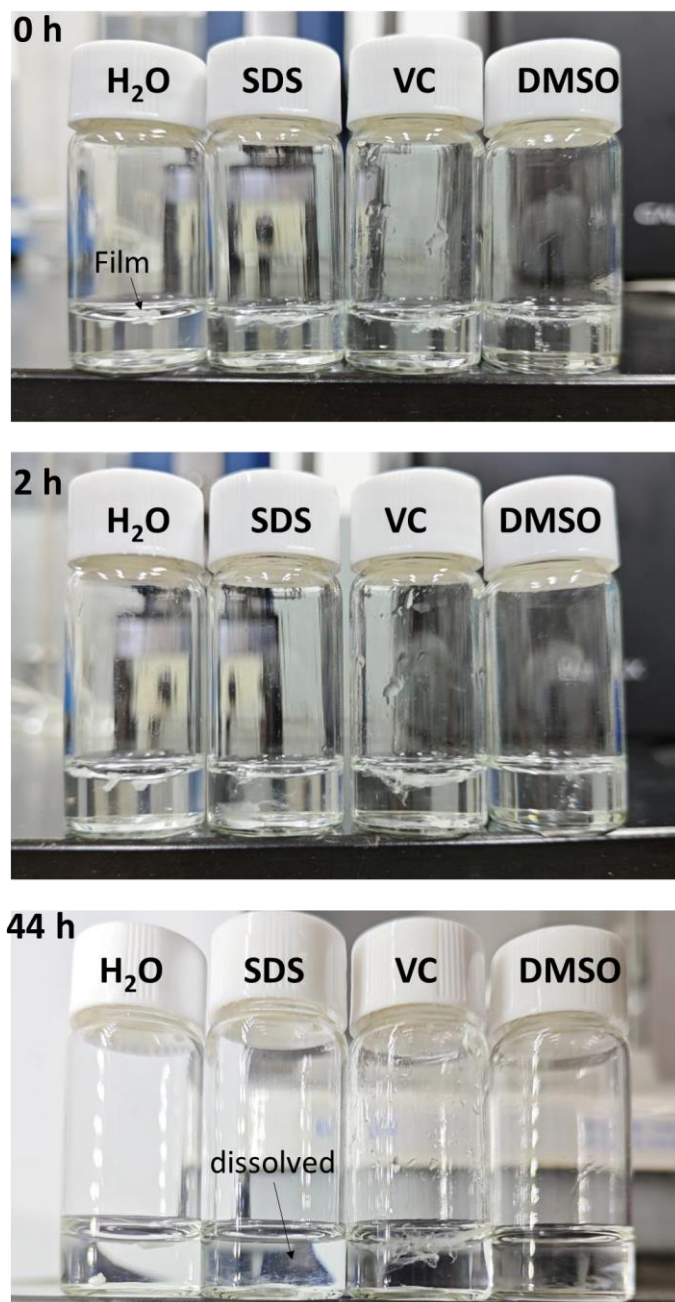


Figure S28. Digital photos of R-Lyz nanofilm soaked in different solution for different times. SDS concentration 2%wt; VC concentration, 500 mM.

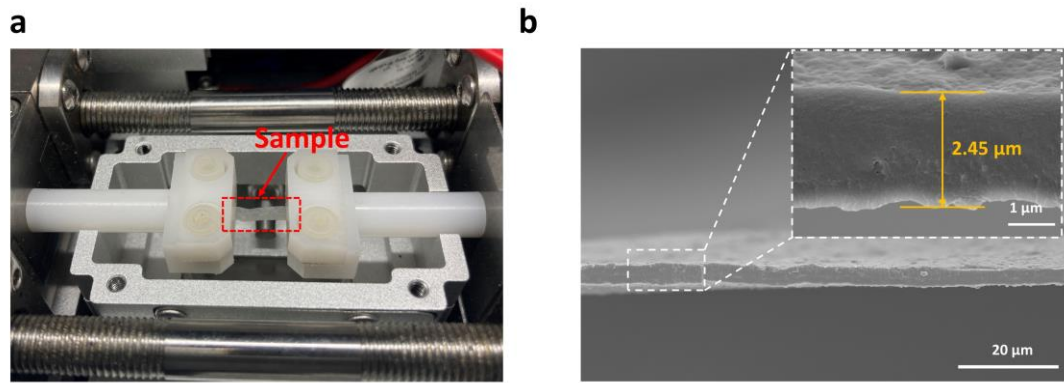


Figure S29. Mechanical property analysis of Janus nanofilm. (a) Tension test of multi-layer Janus nanofilm; (b) Thickness analysis of the multi-layer Janus nanofilm by SEM cross-section image.

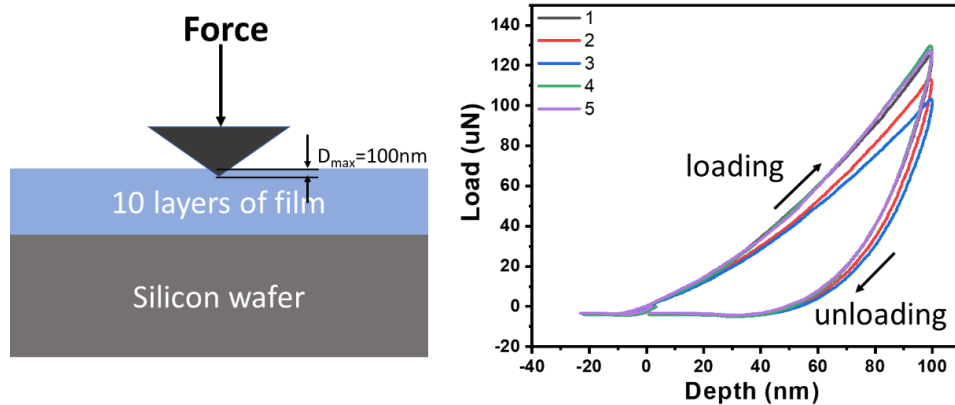
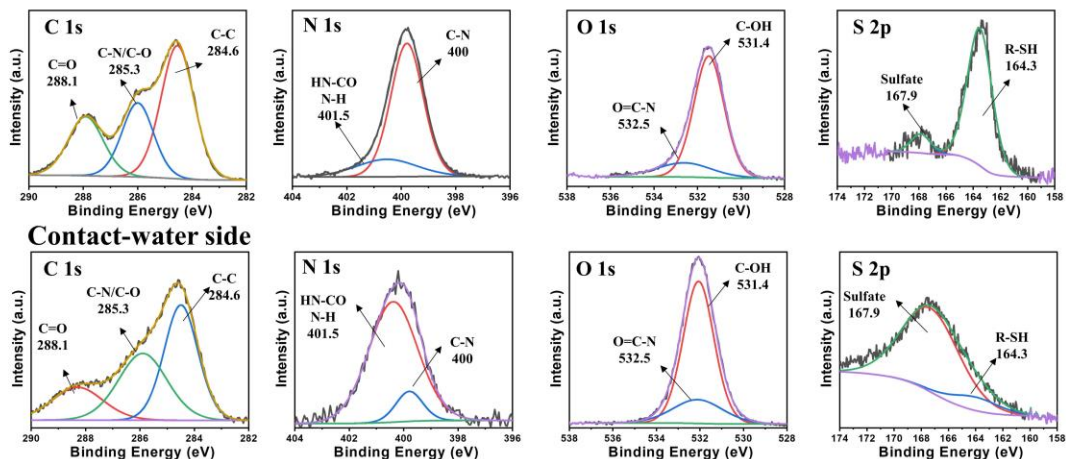


Figure S30. Nanoindentation analysis of Janus nanofilm. Illustration of nanoindentation test and associated load-depth compliance curve.

a Contact-air side



Contact-water side

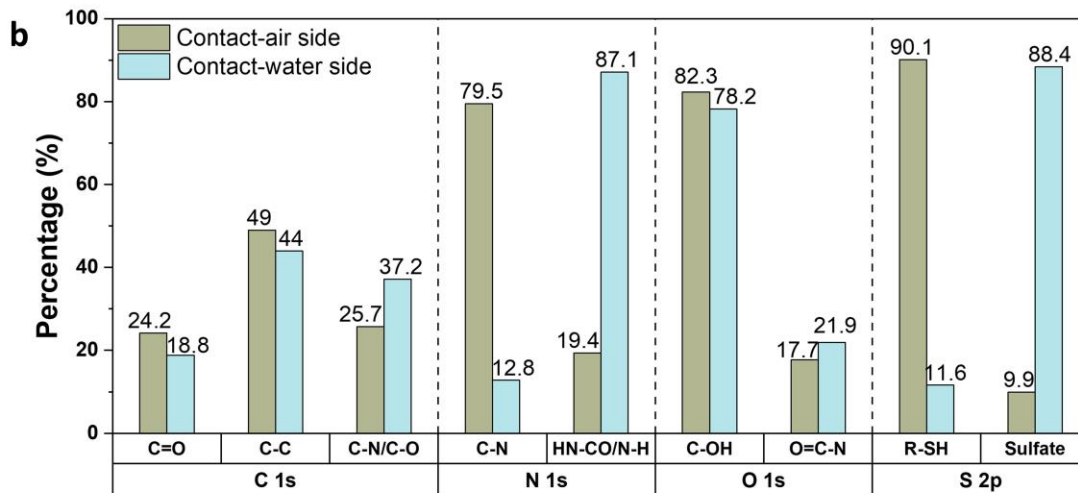
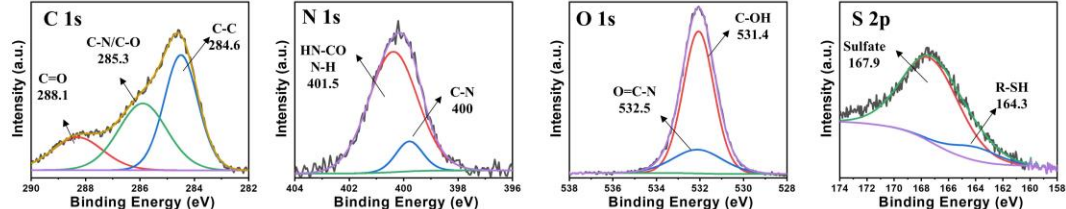


Figure S31. Component analysis of Janus nanofilm. (a) Grazing angle (45°) XPS spectra of Janus nanofilm at AWI; (b) The proportion of each group after XPS peak fitting.

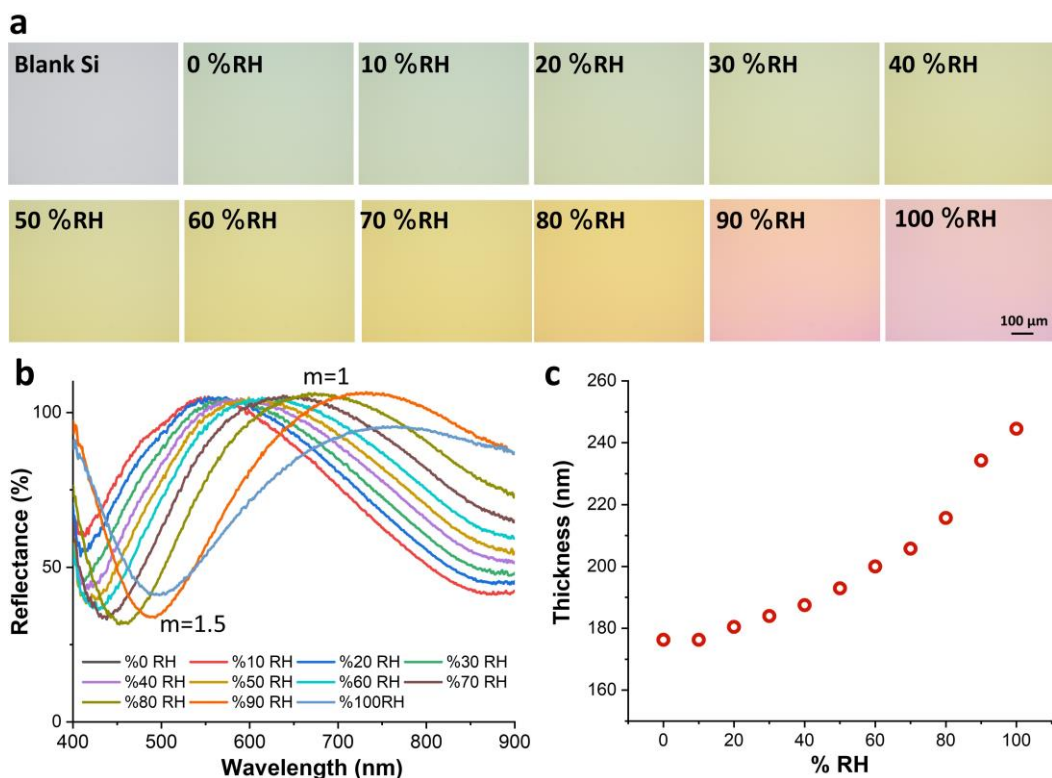


Figure S32. Film swelling property analysis. (a) Digital images of a Janus protein film (dry thickness ~ 176 nm) on silicon wafer under different relative humidity (%RH); (b) Reflectance spectrum of the film under various %RH; (c) Film thickness change against %RH.

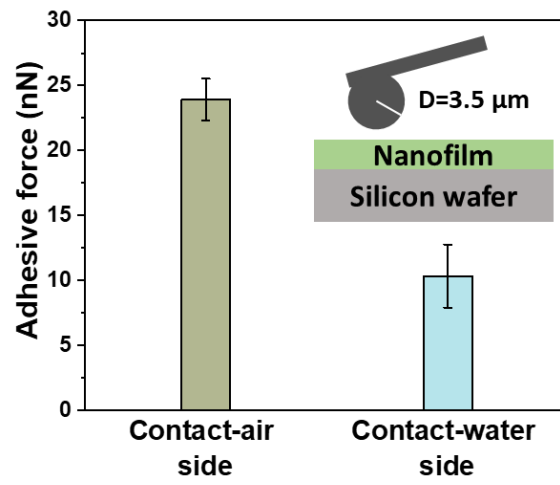


Figure 33. Adhesive force analysis of the Janus nanofilm (measured by AFM with SiO₂ sphere tip).

References

1. Steinigeweg, D. & Schlücker, S. Monodispersity and size control in the synthesis of 20 – 100 nm quasi-spherical silver nanoparticles by citrate and ascorbic acid reduction in glycerol – water mixtures. *Chem. Commun.* **48**, 8682 (2012).
2. Biancalana, M. & Koide, S. Molecular mechanism of Thioflavin-T binding to amyloid fibrils. *Biochimica Et Biophysica Acta (Bba) - Proteins and Proteomics.* **1804**, 1405-1412 (2010).
3. Aliyan, A., Cook, N. P. & Martí, A. A. Interrogating Amyloid Aggregates using Fluorescent Probes. *Chem. Rev.* **119**, 11819-11856 (2019).
4. Kang, Y. et al. Conformation and persistence length of chitosan in aqueous solutions of different ionic strengths via asymmetric flow field-flow fractionation. *Carbohydr. Polym.* **271**, 118402 (2021).
5. Arnaudov, L. N. & de Vries, R. Thermally Induced Fibrillar Aggregation of Hen Egg White Lysozyme. *Biophys. J.* **88**, 515-526 (2005).
6. Muramoto, S. et al. ToF-SIMS Analysis of Adsorbed Proteins: Principal Component Analysis of the Primary Ion Species Effect on the Protein Fragmentation Patterns. *J. Phys. Chem. C.* **115**, 24247-24255 (2011).
7. Delaglio, F. et al. NMRPipe: A multidimensional spectral processing system based on UNIX pipes. *J. Biomol. Nmr.* **6**, 277-293 (1995).
8. Johnson, B. A. & Blevins, R. A. NMR View: A computer program for the visualization and analysis of NMR data. *J. Biomol. Nmr.* **4**, 603-614 (1994).
9. Anthis, N. J. & Clore, G. M. Sequence - specific determination of protein and peptide concentrations by absorbance at 205 nm. *Protein. Sci.* **22**, 851-858 (2013).
10. Provencher, S. W. & Gloeckner, J. Estimation of globular protein secondary structure from circular dichroism. *Biochemistry.* **20**, 33-37 (1981).
11. van Stokkum, I. H. M., Spoelder, H. J. W., Bloemendal, M., van Grondelle, R. & Groen, F. C. A. Estimation of protein secondary structure and error analysis from circular dichroism spectra. *Anal. Biochem.* **191**, 110-118 (1990).
12. Compton, L. A. & Johnson, W. C. Analysis of protein circular dichroism spectra for secondary structure using a simple matrix multiplication. *Anal. Biochem.* **155**, 155-167 (1986).
13. Sreerama, N. & Woody, R. W. A Self-Consistent Method for the Analysis of Protein Secondary Structure from Circular Dichroism. *Anal. Biochem.* **209**, 32-44 (1993).
14. Sreerama, N., Venyaminov, S. Y. & Woody, R. W. Estimation of the number of α - helical and β - strand segments in proteins using circular dichroism spectroscopy. *Protein. Sci.* **8**, 370-380 (1999).
15. Van Der Spoel, D. et al. GROMACS: fast, flexible, and free. *J. Comput. Chem.* **26**, 1701-1718 (2005).
16. Berendsen, H. J., Postma, J. P., van Gunsteren, W. F. & Hermans, J. Interaction models for water in relation to protein hydration. *Intermolecular forces*: Springer; 1981. pp. 331-342.
17. Itoh, S. G., Yagi-Utsumi, M., Kato, K. & Okumura, H. Effects of a Hydrophilic/Hydrophobic Interface on Amyloid- β Peptides Studied by Molecular Dynamics Simulations and NMR Experiments. *The Journal of Physical Chemistry B.* **123**, 160-169 (2018).
18. Hess, B., Bekker, H., Berendsen, H. J. & Fraaije, J. G. LINCS: a linear constraint solver for

- molecular simulations. *J. Comput. Chem.* **18**, 1463-1472 (1997).
19. Darden, T., York, D. & Pedersen, L. Particle mesh Ewald: An $N \cdot \log(N)$ method for Ewald sums in large systems. *J. Chem. Phys.* **98**, 10089-10092 (1993).
 20. Berendsen, H. J., Postma, J. V., van Gunsteren, W. F., DiNola, A. & Haak, J. R. Molecular dynamics with coupling to an external bath. *J. Chem. Phys.* **81**, 3684-3690 (1984).
 21. Hou, T., Wang, J., Li, Y. & Wang, W. Assessing the Performance of the MM/PBSA and MM/GBSA Methods. 1. The Accuracy of Binding Free Energy Calculations Based on Molecular Dynamics Simulations. *J. Chem Inf. Model.* **51**, 69-82 (2011).
 22. Krieger, E. & Vriend, G. YASARA View—molecular graphics for all devices—from smartphones to workstations. *Bioinformatics.* **30**, 2981-2982 (2014).
 23. Perez-Rea, D., Zielke, C. & Nilsson, L. Co-elution effects can influence molar mass determination of large macromolecules with asymmetric flow field-flow fractionation coupled to multiangle light scattering. *J. Chromatogr. A.* **1506**, 138-141 (2017).